



Published in final edited form as:

*J Biomed Nanotechnol.* 2014 September ; 10(9): 1918–1936. doi:10.1166/jbn.2014.1963.

## Functionalized Fullerenes in Photodynamic Therapy

Ying-Ying Huang<sup>1,2</sup>, Sulbha K. Sharma<sup>3</sup>, Rui Yin<sup>1,2,4</sup>, Tanupriya Agrawal<sup>1,2</sup>, Long Y. Chiang<sup>5</sup>, and Michael R. Hamblin<sup>1,2,6,\*</sup>

<sup>1</sup>Wellman Center for Photomedicine, Massachusetts General Hospital, Boston, MA 02114, USA

<sup>2</sup>Department of Dermatology, Harvard Medical School, Boston, MA 02115, USA

<sup>3</sup>Raja Ramanna Centre for Advanced Technology, Indore, MP 452013, India

<sup>4</sup>Department of Dermatology, Southwest Hospital, Third Military Medical University, Chongqing 400038, China

<sup>5</sup>Department of Chemistry, Institute of Nanoscience and Engineering Technology, University of Massachusetts, Lowell, MA 01854, USA

<sup>6</sup>Harvard-MIT Division of Health Sciences and Technology, Cambridge, MA 02139, USA

### Abstract

Since the discovery of C<sub>60</sub> fullerene in 1985, scientists have been searching for biomedical applications of this most fascinating of molecules. The unique photophysical and photochemical properties of C<sub>60</sub> suggested that the molecule would function well as a photosensitizer in photodynamic therapy (PDT). PDT uses the combination of non-toxic dyes and harmless visible light to produce reactive oxygen species that kill unwanted cells. However the extreme insolubility and hydrophobicity of pristine C<sub>60</sub>, mandated that the cage be functionalized with chemical groups that provided water solubility and biological targeting ability. It has been found that cationic quaternary ammonium groups provide both these features, and this review covers work on the use of cationic fullerenes to mediate destruction of cancer cells and pathogenic microorganisms *in vitro* and describes the treatment of tumors and microbial infections in mouse models. The design, synthesis, and use of simple pyrrolidinium salts, more complex decacationic chains, and light-harvesting antennae that can be attached to C<sub>60</sub>, C<sub>70</sub> and C<sub>84</sub> cages are covered. In the case of bacterial wound infections mice can be saved from certain death by fullerene-mediated PDT.

### Keywords

Fullerene; Photodynamic Therapy; Reactive Oxygen Species; Cancer; Infections; Electron Transfer; Singlet Oxygen; Cationic Charge

## INTRODUCTION

Photodynamic therapy (PDT) is based on the administration of nontoxic light absorbing dyes called photosensitizers (PS), either systemically, locally or topically, followed by irradiation of harmless visible to near infrared (NIR) light, in the presence of oxygen, leading to the generation of cytotoxic reactive oxygen species (ROS).<sup>1</sup> Dual selectivity of PDT can be obtained by the therapeutic gradient of photosensitizer concentration between tumor and normal tissues and precise delivery of light exposure within the tumor.<sup>2</sup> However, the major limitations of PDT are non-specific cellular uptake of PS by normal cells and short light penetration depth. PDT is a widely recognized valuable treatment option for neoplastic and non-malignant diseases. Recently with the development of fiber-optic systems, light can be delivered accurately into many parts of the body for the treatment of tumors. Therefore, PDT applications have been expanded to many endoscopically accessible tumors, including lung cancer, superficial gastric cancer, head and neck cancer, cervical cancer and bladder cancer. In general, there are a number of advantages for PDT over chemotherapy and radiotherapy: PDT shows no long-term side effects when an effective PS is employed; it is a minimally-invasive procedure with little or no scarring after the site heals as compared to surgery; it can deliver highly targeted precision at the disease site; there can be repeatable treatments at the same site if needed; PDT can be less costly than other cancer treatments; it may take only a short period of time for each session allowing treatment as an outpatient. The main limitation of PDT is its action occurs only at areas where light can reach. This implies that the major sites of tumors treated by PDT are the lining of organs or just under the skin that can be reached by the light source.

## TRADITIONAL PHOTSENSITIZERS

Photosensitizers can be categorized by their chemical structures as porphyrins (tetrapyrroles) and nonporphyrins.<sup>3</sup> First, second or third generation PS are terms further used to label tetrapyrrole-derived PS. Porphyrins are derived from the tetrapyrrole aromatic macrocycle which is a major component of many naturally occurring pigments such as heme, chlorophyll and bacteriochlorophyll. Porphyrins contain a structure with a 22  $\pi$ -electron system which gives rise to their long wavelength absorption of light.<sup>4</sup> Hematoporphyrin (Hp), hematoporphyrin derivative (HpD) and Photofrin are referred to as first generation PS. HpD and Photofrin have been widely used in clinical for cancer.<sup>5</sup> However, the side effects associated with 1st generation PS, such as prolonged skin photosensitization and suboptimal tissue penetration of the 630 nm light have stimulated interest in development of new PS. Second generation of PS are chemically purified or synthetic tetrapyrrole derivatives, which absorb longer wavelength light and cause less skin photosensitization. Some promising second generation photosensitizers have been approved or tested in clinical trials.<sup>6</sup> These include, but are not limited to, palladium-bacteriopheophorbide (TOOKAD),<sup>7</sup> meso-tetrahydroxyphenylchlorin (Foscan<sup>®</sup>, Temoporfin),<sup>8</sup> tin-ethyletiopurpurin (SnET2, Purlytin), Visudyne<sup>®</sup> (verteporfin, benzoporphyrin derivative monoacid ring A, BPD-MA; Novartis Pharmaceuticals), NPe6 (mono-*L*-aspartyl chlorin e6, taporfin sodium, talaporfin, LS11; Light Science Corporation), Levulan<sup>®</sup> (5-aminolevulinic acid, a precursor of protoporphyrin IX),<sup>9</sup> and phthalocyanines (Pc4).<sup>10</sup> The term "third generation PS" refers to the 2nd generation PS bound to carriers such as antibody conjugates<sup>11</sup> liposomes and other targeted

structures for increasing the selectivity for tumor tissues. Although the majority of PS are porphyrin derivatives, non-porphyrin PS are being employed to improve PDT efficacy and minimal side effects. Synthetic, non-naturally-occurring, conjugated or expanded pyrrolic ring systems are another class of non-porphyrin PS, including texaphyrins, porphycenes, phthalocyanines and naphthalocyanines. Other compounds that have been studied as PS are not derived from the tetrapyrrole backbone, but can be classed as miscellaneous dyes including chalcogenopyrylium dyes,<sup>12</sup> phenothiazinium dyes including methylene blue and toluidine blue,<sup>13</sup> Nile blue derivatives,<sup>14</sup> hydroxylated perylenequinones such as hypericin,<sup>15</sup> BODIPY derivatives,<sup>16</sup> squaraines<sup>17</sup> etc. These compounds have provided a new focus to the field of PDT.

It is generally accepted that the characteristics that the ideal PS used against cancer should possess are:

1. single compound with known composition and good stability,
2. preferential uptake and retain in the target tumour tissue,
3. minimal toxicity in the absence of light to prevent harmful side-effect to the surrounding normal tissue,
4. high quantum yield of triplet state and ROS generation and
5. high molar extinction coefficient to minimize the dose of PS needed to achieve the desired PDT effect,
6. intrinsic fluorescence to permit their detection by optical imaging (microscopy) techniques, and
7. high absorbance, particularly in the red part of the spectrum, which leads to a deeper light penetration into the tissues; for instance, the light depth penetration at 500 nm is about 4 mm, whereas at the 600–800 nm range it is about 8 mm<sup>2</sup>.

### Photophysics and Photochemistry of PDT

Most PS have 2 electrons with opposite spins located in an energetically lower energy orbital, the so-called highest occupied molecular orbital (HOMO), in their ground (usually single) state. Absorption of light (photons) leads to an excited singlet state by the elevation of one electron with unchanged spin to a higher energy orbital, called the lowest unoccupied molecular orbital (LUMO).<sup>18</sup> This excited singlet PS is short-lived (nanoseconds) and emits excess energy as fluorescence and/or heat. Alternatively, an excited PS may undergo an intersystem crossing (ISC) by inverting spin of one electron to form a relatively long-lived (microseconds to milliseconds) triplet state.

The excited triplet PS can either decay radiationlessly to the ground state or can survive long enough to transfer its energy to molecular oxygen O<sub>2</sub> (ground triplet state) and produce excited state singlet oxygen (<sup>1</sup>O<sub>2</sub>). This reaction is referred to as a Type II process. A Type I process can also occur whereby the PS reacts directly with neighboring molecules and gains or donates an electron to form a radical. Subsequent electron donation from the PS radical anion to oxygen produces the superoxide anion radical (O<sub>2</sub><sup>-•</sup>). Therefore, the efficient ISC

process giving a high quantum yield of triplet state is essential for the generation of ROS. Strong absorption of light, high triplet state quantum yield (effective ISC) and a long-lived triplet excited state are required to be an ideal PS. However, there has not yet been established a clear relationship between the efficiency of ISC and the chemical structure.

## FULLERENES AS PHOTSENSITIZERS

Besides occupying an important place in biomedicine, nanoparticles have also been shown to have potential to act as a photosensitizing drug in PDT. Fullerenes are considered to have advantages as potential PS on the basis of certain favorable PDT characteristics when compared to conventional PS with the tetrapyrrole structure.<sup>19</sup> The fullerenes are known for their photostability, a prerequisite to behave as an effective PS, and they undergo relatively less photobleaching than the tetrapyrroles. They can also be modified to get the desired degree lipophilicity by chemical functionalization.<sup>20</sup> There is the option of attaching the light-harvesting antennae to the fullerenes to increase the quantum yield of production of ROS. Fullerenes can self-assemble into vesicles called fullerosomes that can act as multivalent drug delivery vehicles with the possibility of different targeting properties.<sup>21</sup>

Fullerenes have been said to offer “a wide open playing field to chemists”<sup>22</sup> by providing synthetic opportunities to attach a wide variety of hydrophilic or amphiphilic side chains or fused-ring structures to the spherical C<sub>60</sub> core.<sup>22</sup> Furthermore, fullerenes have hollow interiors, where other atoms, ions or small clusters can be entrapped and form endohedral fullerenes. Those fullerenes that encapsulate metal atoms are called endohedral metallofullerenes.<sup>23</sup> Hydroxylation (attaching OH-groups) is the most common functionalization, which renders the molecule more hydrophilic,<sup>24</sup> but other polar adducts will also have the same effect.<sup>25</sup>

There are also several unfavorable characteristics of fullerenes for PDT, but by applying different strategies they can be overcome. The main absorption of fullerenes occurs in the UV, blue and green regions of the spectrum while the absorption of tetrapyrrole PS (such as chlorins, bacteriochlorins, and phthalocyanines) shows substantial peaks in the red or far-red regions where the penetration of light into tissue is much deeper. This major disadvantage of fullerenes however can be overcome in several ways, for example by chemical attachment of one or more red-wavelength absorbing antennae onto a C<sub>60</sub> cage.<sup>26</sup> The absorption of many light photons simultaneously can be achieved by the attachment of multiple light-harvesting antennae on one C<sub>60</sub> cage. The unfavorable absorption spectrum of fullerenes can also be overcome by using optical clearing agents to the tissue<sup>27–30</sup> or by using two-photon excitation where two NIR photons are simultaneously delivered in a very short pulse to be equivalent to one photon of twice the energy and shorter wavelength.<sup>31–35</sup>

### Photophysics and Photochemistry of Fullerenes and Derivatives

Fullerenes with attached side chains, called “functionalized fullerenes,” are known to demonstrate high efficiency in the formation of singlet oxygen, hydroxyl radicals and superoxide anions, which are considered as effective mediators of PDT. The photophysics of fullerenes is quite favorable for PDT. The absorption spectra of a typical set of mono-substituted, bis-substituted and tris-substituted fullerenes show almost monotonic decay

between 300 and 700 nm.<sup>20</sup> When C<sub>60</sub> is irradiated with visible light, it is excited from the S<sub>0</sub> ground state to a short-lived (<1.3 ns) S<sub>1</sub> excited state. The S<sub>1</sub> state quickly decays to triplet state. The triplet yield is 1 and the lifetime is as long as 50–100 μs. By energy transfer mechanism (Type II) there is the generation of singlet oxygen (<sup>1</sup>O<sub>2</sub>) by quenching of fullereryl T<sub>1</sub> state in the presence of dissolved molecular oxygen. At 532 nm excitation the singlet oxygen quantum yield (Φ) for this process is close to theoretical maximum, 1.0.<sup>36</sup> Calculations in 1986 by Haddon et al. had indicated that the lowest unoccupied molecular orbital (LUMO) of C<sub>60</sub> would be low-lying, triply degenerate, and, hence, capable of accepting up to 6 electrons.<sup>37</sup> The pristine C<sub>60</sub> itself alone is not a good PS due to the very weak absorption of visible light and water insolubility. However, C<sub>60</sub> is an ideal spin converter due to its efficient inherent ISC and a low S<sub>1</sub> state energy level (about 1.72 eV). When a visible-light-harvesting antenna is attached onto C<sub>60</sub> to produce C<sub>60</sub>-dyads, it turns out to be a potentially ideal PS.<sup>38</sup> Figure 1 shows a schematic outline centered upon a Jablonski diagram of PDT mediated by fullerene and its derivatives.

Both pristine and functionalized fullerenes have the potential to produce ROS after illumination.<sup>39</sup> The ROS produced by fullerene derivatives during illumination are inclined towards Type I photochemical products (superoxide radical, hydroxyl radical, lipid hydroperoxides, and hydrogen peroxide), compared to the standard Type II ROS (singlet oxygen) for most PS. During this process they are able accept electrons very efficiently as many as six to each C<sub>60</sub> cage.<sup>40,41</sup> It is thought that the reduced fullerene triplet or radical anion can transfer an electron to molecular oxygen, forming the superoxide anion radical.<sup>42</sup> One apparent incongruity that arises in this area needs to be addressed. It is a well-known fact that fullerenes can act as antioxidants, and that C<sub>60</sub> and derivatives can act as scavengers of ROS in the absence of light. One clue that might explain this inconsistency was proposed in 2009, by Andrievsky et al.<sup>43</sup> who showed that the major mechanism by which hydrated C<sub>60</sub> can inactivate the highly reactive ROS, hydroxyl radical, not by covalently scavenging the radicals but rather by action of the coat of “ordered water” that was linked with the fullerene nanoparticle.<sup>44</sup> One of the explanations is that hydroxyl radicals can be slowed down or trapped for a sufficient time allowing the two radicals to react with each other, which produce the comparatively less-reactive ROS, hydrogen peroxide. However, the mechanism may be significantly different with more water-compatible C<sub>60</sub> derivatives.<sup>45</sup>

## DESIGN OF FULLERENE DERIVATIVES

One of the concerns that have been raised about the use of fullerenes concerns their biodegradability, as nanostructures have the possibility of accumulation in the body during blood circulation or in the environment after use.<sup>46</sup> Though it has been shown that pristine C<sub>60</sub> is nontoxic its insolubility and its pronounced tendency to aggregate decreases its potential to be useful in biomedicine. Many strategies have been demonstrated or applied to either solubilize or modify fullerenes for improving their utility in drug-delivery and medical applications. The following approaches: liposomes;<sup>47–49</sup> micelles;<sup>50,51</sup> dendrimers;<sup>52,53</sup> PEGylation;<sup>53–56</sup> self-nanoemulsifying systems (SNES);<sup>57–60</sup> encapsulation in cyclodextrins.<sup>47, 61, 62</sup> have all been explored by various groups throughout the world to overcome this problem with fullerenes.

It is known that cationic functional groups provide good solubility for molecules of diverse structures and also have the potential to bind to the anionic residues present on cancer cells and also on the bacterial cell wall via static charge interactions. For these reasons cationic groups can be considered a good choice for attachment on the fullerene cage. A number of chemical functionalization techniques for derivatizing fullerenes have been evaluated.<sup>63, 64</sup> Among them, general suitable methods for the preparation of cationic fullerene derivatives include cyclopropanation<sup>65</sup> e.g.,  $C_{60}[\text{>M}(\text{C}_3\text{N}_6^+\text{C}_3)_2]-(\text{I}^-)_{10}$  (LC14, Fig. 2(a))<sup>66, 67</sup> and  $C_{70}[\text{>M}(\text{C}_3\text{N}_6^+\text{C}_3)_2]-(\text{I}^-)_{10}$  (LC17, Fig. 2(b))<sup>68</sup> and pyrrolidination e.g., quaternized dimethylpyrrolidinium fulleranyl monoadduct (BF4,<sup>20</sup> Fig. 2(c)) and trisadduct (BF6,<sup>69</sup> Fig. 2(d)) and structures such as LC22,  $C_{60}[\text{>DPAF}(\text{MN}_6^+\text{C}_3)_2]-(\text{I}^-)_{10}$ , and LC24,  $C_{70}[\text{>M}(\text{C}_3\text{N}_6^+\text{C}_3)_2]-(\text{I}^-)_{20}$ .<sup>70, 71</sup>

The cyclopropanation reaction of  $C_{60}$  functionalization was recently applied to attach a highly complex decacationic moiety to the fullerene cage leading to the formation of fullerenes bearing ten positive charges. The decacationic functional moieties of  $C_{60}$ ,  $C_{70}$ , and  $C_{84}\text{O}_2$  fullerenes were designed to increase both the water-solubility and provide surface binding interactions with *-D-Ala-D-Ala* residues of the bacteria cell wall by incorporating multiple H-bonding interactions and positive quaternary ammonium charge to bind to anionic lipopolysaccharides and lipoteichoic acids.<sup>70</sup> The structure included two esters and two amide moieties to give a sufficient number of carbonyl and  $-\text{NH}$  groups in a short length of  $\sim 20$  Å to provide effective multi-binding sites with the presence of a well-defined water-soluble pentacationic moiety  $\text{C}_3\text{N}_6^+\text{C}_3-\text{OH}$  at each side of the arm. A similar reaction sequence with a malonate precursor arm  $\text{M}(\text{C}_3\text{N}_6\text{C}_3)_2$  was also employed in the preparation of  $C_{70}[\text{>M}(\text{C}_3\text{N}_6^+\text{C}_3)_2][\text{>M}(\text{C}_3\text{N}_6\text{C}_3)_2]-(\text{I}^-)_{10}$  (LC18, Fig. 2(e)),  $C_{84}\text{O}_2[\text{>M}(\text{C}_3\text{N}_6^+\text{C}_3)_2]-(\text{I}^+)_{10}$  (LC19, Fig. 2(f)),  $C_{84}\text{O}_2[\text{>M}(\text{C}_3\text{N}_6^+\text{C}_3)_2][\text{>M}(\text{C}_3\text{N}_6\text{C}_3)_2]-(\text{I}^-)_{10}$  (LC20, Fig. 2(g)).<sup>67</sup>

To circumvent the shortcoming of weak absorption of light at visible wavelengths, a variety of highly fluorescent donor chromophore antennae have been covalently attached to the fullerene, such as porphyrins.<sup>72</sup> Fullerene-porphyrin hybrids are more efficient in terms of singlet oxygen generation and also have improved cell penetration.

Dialkyldiphenylaminofluorene (DPAF- $C_{2M}$ , shown in Fig. 2(h)) is also a light-harvesting donor chromophore antenna that can be attached to the  $C_{60}$  cage to facilitate ultrafast intramolecular energy- and electron-transfer from the donor antenna to  $C_{60}$  and can therefore be used to enhance PDT efficacy.<sup>73</sup> DPAF- $C_{2M}$  was constructed to have increased optical absorption at 400 nm and also possessed good two-photon absorption (2PA) cross-sections in the NIR wavelengths. Later another set derivatives  $C_{60}(\text{>CPAF-}C_{2M})$  (Fig. 2(i)) was formed by structural modification via chemical conversion of the keto group in  $C_{60}(\text{>DPAF-}C_{2M})$  to a stronger electron-withdrawing 1,1-dicyanoethylenyl (DCE) unit. This structural modification induced a large bathochromic shift of ground-state absorption of CPAF- $C_{2M}$  moieties beyond 450–550 nm and an increased electronic polarization of the molecule. The modification also led to a large bathochromic shift of the major band in visible spectrum giving measureable absorption up to 600 nm and extended the

photoresponsive capability of C<sub>60</sub>-DCE-DPAF nanostructures to longer red wavelengths than C<sub>60</sub>(>DPAF-C<sub>2M</sub>).

It was reported that the majority of the HOMO electron density was delocalized over the dialkyldiphenylaminofluorene (DPAF-C<sub>n</sub>) moiety, whereas the LUMO electron density was located on the C<sub>60</sub> spheroid.<sup>74</sup> Therefore charge-separated states may be generated by intramolecular electron-transfer between the diphenylaminofluorene donor and C<sub>60</sub> > acceptor moieties during the photoexcitation process.

Intramolecular formation of transient charge-separated states is crucial for generation of radical ROS, initially with O<sub>2</sub><sup>-•</sup> and subsequently HO<sup>•</sup>. C<sub>60</sub><sup>-•</sup> (>CPAF<sup>+•</sup>-C<sub>n</sub>) is the most stable charge-separated state in polar solvents, including H<sub>2</sub>O.<sup>74</sup> In nonpolar solvents, the intramolecular energy-transfer event that produces <sup>3</sup>C<sub>60</sub><sup>\*</sup> (>CPAF-C<sub>n</sub>) transient state dominates with nearly 6-fold higher generation of singlet O<sub>2</sub> compared to <sup>3</sup>C<sub>60</sub><sup>\*</sup> (>DPAF-C<sub>n</sub>).

### Examples of the Synthesis of Monocationic and Polycationic Fullerene Derivative

As mentioned above cationic functional groups are generally considered as the addend of choice for attachment on the fullerene cage due to their potential surface binding contact with anionic residues of the bacteria cell wall via static charge interactions. A systematic trend to increase the number of positive charges per fullerene cage was described in a recent report<sup>75</sup> to maximize such interactions and use them as the approach for targeting bacteria having a significant density of anionic residues at the cell wall surface. A number of chemical functionalization methods of fullerenes have been reviewed.<sup>64, 76-78</sup> Among them, common convenient methods for the preparation of cationic fullerene derivatives include cyclopropanation<sup>79</sup> and pyrrolidination<sup>80</sup> reactions due to their high consistency allowing product reproducibility. Examples of the latter were given in the preparation of quaternized dimethylpyrrolidinium [60] fullerene monoadduct (BF4) and trisadduct (BF6).<sup>81, 82</sup> In a typical reaction condition, C<sub>60</sub> was treated with 1.0 or 3.0 equivalent of *N*-methylglycine (sarcosine) and paraformaldehyde in toluene at the refluxing temperature to afford either mono-*N*-methylpyrrolidino[60] fullerene (BF4) or a large number of regioisomers of tris(*N*-methylpyrrolidino)[60] fullerene (BF6) derivatives, as shown in Figure 3. Upon quaternization of these intermediates using methyl iodide as the methylation agent, corresponding monocationic and tricationic products as BF4 and BF6 were obtained, respectively.

Similarly, the reaction of C<sub>60</sub> in toluene with either 1.0 or 2.0 equivalent of azomethine ylide produced by piperazine-2-carboxylic acid dihydrochloride dissolved in methanol and triethylamine in the presence of 4-pyridinecarboxaldehyde at the refluxing temperature gave the corresponding mono-piperazinopyrrolidino[60] fullerene or a number of regioisomers of bis(piperazinopyrrolidino)[60] fullerene derivatives. Quaternization of both intermediates with methyl iodide led to the corresponding monocationic and dicationic products as BF22 and BF24 (Fig. 3), respectively.

In the case of cyclopropanation reaction of  $C_{60}$  as the functionalization method, it was applied recently for the attachment of a highly complex decacationic moiety to the fullerene cage leading to the formation of  $C_{60}[>M(C_3N_6^+C_3)_2]$  and  $C_{70}[>M(C_3N_6^+C_3)_2]$ .<sup>83</sup> In this reaction, a malonate precursor arm was applied to include two esters and two amide moieties, for a sufficient number of carbonyl and  $-NH$  groups in a short length of  $\sim 20$  Å, with a well-defined water-soluble pentacationic moiety  $N_6^+C_3$  at each side of the arm for making effective multi-binding sites to the cell wall. The precursor  $N_6^+C_3$  was reported to be a common synthon for the structural modification of PDT nanomedicines. It was derived from the quaternization of  $N,N',N,N,N,N$ -hexapropyl-hexa(aminoethyl)amine precursor  $N_6C_3$ . The best method for the preparation of  $C_{60}[>M(C_3N_6^+C_3)_2]$  and  $C_{70}[>M(C_3N_6^+C_3)_2]$  was depicted in Figure 4 to begin with a well-defined fullerene monoadduct derivatives, such as di(*tert*-butyl)fullerenyl malonates  $C_{60}[>M(t-Bu)_2]$  and  $C_{70}[>M(t-Bu)_2]$ , respectively, followed by facile transesterification reaction with the well-characterized tertiary-amine precursor arm moiety, 4-hydroxy- $[N,N',N,N,N,N$ -hexapropyl-hexa(aminoethyl) butanamide ( $C_3N_6C_3-OH$ ) using trifluoroacetic acid as the catalytic reagent to afford protonated quaternary ammonium trifluoroacetate salt  $C_{70}[>M(C_3N_6^+C_3H)_2]$ . Conversion of this salt to  $C_{70}[>M(C_3N_6^+C_3)_2]$  was accompanied by neutralization of trifluoroacetic acid by sodium carbonate and subsequent quaternization by methyl iodide to give decacationic quaternary ammonium iodide salts. A similar conversion procedure was applied for the case of  $C_{60}[>M(C_3N_6^+C_3)_2]$ . This synthesis represented the first examples of decacationic fullerene monoadducts to incorporate a well-defined high number of cation without the use of multiple addend attachments to preserve the intrinsic photophysical properties of fullerene cages.

### Synthesis of Hexa-Anionic Fullerene Derivatives

Fullerene molecules are highly hydrophobic. Pristine  $C_{60}$  can be dispersed into aqueous medium in a micelle form with the application of surfactants. However, the micelle structure may not be stable enough in biological environment. In a recent report, a strategy of creating a micelle formed from surfactants covalently bonded directly onto the fullerene cage was illustrated by the synthesis of hexa(sulfo-*n*-butyl)- $C_{60}$  ( $FC_4S$ ) leading to structurally stable molecular micelles in  $H_2O$ .<sup>84</sup> The synthesis involved the use of hexaanionic  $C_{60}$  ( $C_{60}^{6-}$ ) chemistry<sup>85</sup> for attaching six sulfo-*n*-butyl arms on  $C_{60}$  in one-pot reaction, as shown in Figure 5.

It was found that molecular self-assemblies of  $FC_4S$  resulted in the formation of nearly monodisperse spheroidal nanospheres with the sphere radius of gyration  $R_g \approx 19$  Å, where the major axis  $\approx 29$  Å and the minor axis  $\approx 21$  Å for the ellipsoid-like aggregates, or an estimated long sphere diameter of 60 Å [the radius =  $(5/3)^{1/2}R_g$ ] for the aggregates, as determined by small angle neutron scattering (SANS) in  $D_2O$  and small angle X-ray scattering (SAXS) in  $H_2O$ .<sup>86</sup> This radius of gyration was found to remain relatively constant over a concentration range from 0.35 to 26 mM in  $H_2O$ , revealed strong hydrophobic interaction between core fullerene cages overcoming loose charge repulsion at the surface of the molecular micelle. It allowed the nanosphere formation at a low concentration despite of

steric hindrance and high hydrophilicity arising from of 6 sulfo-*n*-butyl arms surrounding C<sub>60</sub>. Based on the SANS data, the mean number of FC<sub>4</sub>S molecules for the nanosphere was determined to be 6.5± 0.7 that led to the elucidation of its nanocluster structure with each FC<sub>4</sub>S molecule located at the vertex of an octahedron shaped nanosphere shown in Figure 6.<sup>85</sup>

### Synthesis of Chromophore-Linked Fullerene Derivatives

Optical absorption of C<sub>60</sub> is strong in UVA and weak in most of visible range. To circumvent this shortcoming, a reported approach was described to use the light-harvesting donor chromophore antenna attachment at a very close vicinity of C<sub>60</sub> cage, within a contact distance of 2.6–3.5 Å, to facilitate ultrafast intramolecular energy- and electron-transfer from the donor antenna to C<sub>60</sub> for enhancing PDT efficacy.<sup>73</sup> A specific donor antenna, namely, dialkyldiphenylaminofluorene DPAF-C<sub>*n*</sub> was first introduced to give an increased optical absorption at 400 nm and later being modified by replacing the keto moiety of DPAF-C<sub>*n*</sub> via a highly electron-withdrawing 1,1-dicyanoethylenyl (DCE) bridging group that resulted in dark burgundy-red C<sub>60</sub>(>CPAF-C<sub>*n*</sub>) derivatives. This structural modification was found to induce a large bathochromic shift of ground-state absorption of CPAF-C<sub>*n*</sub> moieties beyond 450–550 nm.

Preparation of C<sub>60</sub>(>CPAF-C<sub>2M</sub>), as an example, was made by Friedel-Craft acylation of 9,9-dimethoxyethyl-2-diphenylaminofluorene with bromoacetyl bromide in the presence of AlCl<sub>3</sub> to yield 7-bromoacetyl-9,9-dimethoxyethyl-2-diphenylaminofluorene, followed by cyclopropanation reaction with C<sub>60</sub>, as shown in Figure 7. The resulting product C<sub>60</sub>(>DPAF-C<sub>2M</sub>) was then further treated with malononitrile and pyridine in the presence of titanium tetrachloride in dry toluene to yield C<sub>60</sub>(>CPAF-C<sub>2M</sub>) after chromatographic purification.

### Photochemistry and Photophysics of Fullerenyl Molecular Micelles and Chromophore-Fullerene Conjugates

Photoexcitation of C<sub>60</sub> and fullerene derivatives induces a singlet fullerenyl excited state that is transformed to the corresponding triplet excited state, via intersystem energy crossing, with nearly quantitative efficiency.<sup>41</sup> Subsequent energy transfer from the triplet fullerene derivatives to molecular oxygen produces singlet molecular oxygen in aerobic media. This photocatalytic effect becomes one of key mechanisms in photodynamic treatments using fullerene derivatives as photosensitizers. However, a high degree of functionalization on C<sub>60</sub> for the enhancement of solubility and compatibility in biomedicine resulted in a progressive decrease of the singlet oxygen production quantum yield [ $\Phi(^1\text{O}_2)$ ]. Examples were given by Bingel-type malonic acid, C<sub>60</sub>[C(COOH)<sub>2</sub>]<sub>*n*</sub>, and malonic ester, C<sub>60</sub>[C(COOEt)<sub>2</sub>]<sub>*n*</sub>, [60] fullerene adducts,<sup>87</sup> showing a decreasing trend of  $\Phi(^1\text{O}_2)$  as the number of addends (*n*) increases. When the number *n* reached 6 for a hexaadduct, its  $\Phi(^1\text{O}_2)$  value declined to only 13% or less of that for C<sub>60</sub>.<sup>88</sup> However, it was not the case for molecular micellar FC<sub>4</sub>S, a relatively high singlet oxygen production quantum yield for FC<sub>4</sub>S may indicate its unique electronic features in difference with Bingel-type malonic hexaadducts of C<sub>60</sub>.<sup>85</sup> The efficiency was substantiated by direct detection of <sup>1</sup>O<sub>2</sub> emission at 1270 nm upon photoirradiation of self-assembled FC<sub>4</sub>S nanospheres at 500–600 nm.

In the cases of light-harvesting electron-donor chromophore assisted fullerene conjugate systems, such as  $C_{60}(>>CPAF-C_n)$  derivatives, their photophysical properties involve the primary photoexcitation events of either the fullerene moiety at UV wavelengths or the DPAF- $C_n$  moiety at both UV and visible wavelengths up to 600 nm.<sup>73</sup> Much higher optical absorption capability of DPAF- $C_n$  than the  $C_{60}>$  cage in visible wavelengths enables the former moiety to serve as a light-harvesting antenna. Accordingly, formation of the photoexcited  ${}^1(DPAF)^*-C_n$  moiety should be considered as the early event in the photophysical process. Alteration of the keto group of  $C_{60}(>>DPAF-C_n)$  to the 1,1-dicyanoethylenyl group of  $C_{60}(>>CPAF-C_n)$  effectively extended its photoresponsive region to longer red wavelengths. Photoexcitation processes of  $C_{60}(>>DPAF-C_n)$  and  $C_{60}(>>CPAF-C_n)$  pump an electron from their highest occupied molecular orbital (HOMO) to the lowest unoccupied molecular orbital (LUMO). By the molecular orbital calculation and energy minimization, the majority of the HOMO electron density was reported to be delocalized over the dialkyldiphenylaminofluorene (DPAF- $C_n$ ) moiety, whereas the LUMO electron density was located on the  $C_{60}$  spheroid, and therefore  $C_{60}^{-\bullet}(>>CPAF^{+\bullet}-C_n)$  was suggested as the most stable charge-separated (CS) state in polar solvents, including  $H_2O$ .<sup>74</sup> These charge-separated states may be generated by photoinduced intramolecular electron-transfer between the diphenylaminofluorene donor and  $C_{60}>$  acceptor moieties. The process effectively quenches fluorenyl fluorescence that can be observed in the most of  $C_{60}(>>DPAF-C_n)$  and  $C_{60}(>>CPAF-C_n)$  monoadducts. Even during energy-transfer events of  $C_{60}(>>CPAF-C_n)$ , normally favorable in non-polar solvents, observed short fluorescence lifetime of the model compound  ${}^1CPAF^*-C_9$  (241 ps) as compared with that of the keto analogous Br- ${}^1DPAF^*-C_9$  (2125 ps) may be indicative of a facile photoinduced intramolecular charge polarization process forming the corresponding  $[C=C(CN)_2]^{-\bullet}-DPAF^{+\bullet}-C_9$  charge-separated state that will facilitate the formation of  $C_{60}^{-\bullet}(>>CPAF^{+\bullet}-C_n)$  in the subsequent electron-transfer event.

## ANTICANCER EFFECT OF FULLERENE-PDT

There have been various studies demonstrating fullerene induced *in-vitro* phototoxicity in cells. It is considered that one condition for any PS to produce cell killing after illumination, is that the PS should really be taken up inside the cell, as the production of ROS outside the cell will not be enough to produce cell death unless it is produced in extremely large amounts. One of the limitations for the study of the uptake of fullerenes into cells is their non-fluorescent nature that limits the use of fluorescence microscopy to study the localization in cells. Some strategies though have been adopted to overcome this limitation, such as the use of radiolabeled fullerene that has been prepared to study the uptake. Indirect immunofluorescence staining with antibodies has been used to show the localization of fullerene in mitochondria and other intracellular membranes.<sup>89</sup> Recently energy-filtered transmission electron microscopy and electron tomography was used to visualize the cellular uptake of pristine  $C_{60}$  nanoparticulate clusters in the plasma membrane, lysosomes and in the nucleus of cells.<sup>90</sup>

### ***In Vitro* Anti-Cancer PDT with Fullerenes**

The first report of phototoxicity in cancer cells mediated by fullerenes was in the year 1993. In this study Tokuyama et al.<sup>91</sup> used carboxylic acid functionalized fullerenes at 6.0  $\mu\text{M}$  and white light to produce growth inhibition in cancer cells. Burlaka et al.<sup>92</sup> used pristine  $\text{C}_{60}$  at 10  $\mu\text{M}$  with visible light from a mercury lamp to produce some phototoxicity in Ehrlich carcinoma cells or in rat thymocytes. The cytotoxic and photocytotoxic effects of two water-soluble fullerene derivatives, a dendritic  $\text{C}_{60}$  monoadduct and the malonic acid  $\text{C}_{60}$  trisadduct were tested on Jurkat cells when irradiated with UVA or UVB light.<sup>93</sup> The cell death was mainly caused by membrane damage and it was UV dose-dependent.

New approaches have been tested to overcome the requirement to utilize UV or short-wavelength visible light to activate fullerenes. In one study where two new fullerene-bis-pyrropeophorbide-a derivatives were prepared: a mono-(FP1) and a hexaadduct (FHP1). The  $\text{C}_{60}$  hexaadduct FHP1 had a significant phototoxic activity (58% cell death, after a dose of 400  $\text{mJ}/\text{cm}^2$  of 688 nm light) but the monoadduct FP1 had a very low phototoxicity and only at higher light doses.<sup>94</sup> Nevertheless the activity of both adducts was less than that of pure pyrropeophorbide-a, possibly due to the lower cellular uptake of the adducts.<sup>95</sup>

The hypothesis that fullerenes have the potential to destroy cancer cells by PDT was tested in our group. We have shown that the  $\text{C}_{60}$  molecule mono-substituted with a single pyrrolidinium group (BF4 shown in Fig. 2(c)) is an efficient PS and can mediate killing of a panel of mouse cancer cells.<sup>20</sup> The cells lines used were lung cancer (LLC) and colon cancer (CT26) adenocarcinoma and reticulum cell sarcoma (J774) and the latter showed much higher susceptibility to fullerene mediated phototoxicity possibly due to having an increased uptake because J774 cells behave like macrophages. Besides the exceptionally active BF4, the next group of compounds has only moderate activity (BF2, BF5, and BF6 shown in Fig. 2(d)) against J774 cells showing only some killing even at high fluences, while last two compounds (BF1 and BF3) had no detectable PDT killing up to 80  $\text{J}/\text{cm}^2$ . The indirect measurement of fullerenes uptake was demonstrated by increase in fluorescence of an intracellular probe ( $\text{H}_2\text{DCFDA}$ ) which is specific for the formation of ROS. We also showed the initiation of apoptosis by PDT mediated by BF4 and BF6 in CT26 cells at 4–6 h after illumination. The induction of apoptosis was rapid after illumination which may perhaps suggest that fullerenes are localized in mitochondria, as it has been previously shown with benzoporphyrin derivative.<sup>96–98</sup> The explanation for the mono-pyrrolidinium substituted fullerene as most effective PS most likely linked to its relative hydrophobicity as established by its log P value of over 2. Besides this a single cationic charge on BF4 is in addition expected to play a significant role in determining its relative phototoxicity.

Elisa Milanesio et al.<sup>97</sup> used tetrapyrrole-fullerene conjugates and evaluated PDT effect with a porphyrin- $\text{C}_{60}$  dyad ( $\text{P-C}_{60}$ ) and its metal complex with Zn(II) ( $\text{ZnP-C}_{60}$ ) and compared with 5-(4-acetamidophenyl)-10,15,20-tris(4-methoxyphenyl)porphyrin (P) on Hep-2 human larynx carcinoma cell line. The phototoxicity was dependent on light exposure level with visible light. 80% phototoxicity was observed for  $\text{P-C}_{60}$  after 15 min of light irradiation which was higher as compared to  $\text{ZnP-C}_{60}$ . In case of argon atmosphere also a high

photoactivity was observed with both the dyads. In another paper,<sup>99</sup> the cell death was confirmed to occur by apoptotic mode.

As fullerenes show a relatively slower uptake we incubated the cells for 24h with  $C_{60}[\text{>M}(\text{C}_3\text{N}_6^+\text{C}_3)_2]-(\text{I}^-)_{10}$  (LC14) and  $C_{70}[\text{>M}(\text{C}_3\text{N}_6^+\text{C}_3)_2]-(\text{I}^-)_{10}$  (LC17) (shown in Figs. 2(a) and (b)).  $C_{70}[\text{>M}(\text{C}_3\text{N}_6^+\text{C}_3)_2]-(\text{I}^-)_{10}$  killed cells more effectively than  $C_{60}[\text{>M}(\text{C}_3\text{N}_6^+\text{C}_3)_2]-(\text{I}^-)_{10}$ . On the contrary, the fullerene drug LC14 killed less than 1 log at all fluencies. LC17 that was short of the decatertiary amine chain was less phototoxic than LC18 which possessed an extra deca-tertiary ethyleneamine chain. This exciting result prompted us to carry out studies with new PDT compounds  $C_{84}\text{O}_2[\text{>M}(\text{C}_3\text{N}_6^+\text{C}_3)_2]-(\text{I}^-)_{10}$  (LC19) and  $C_{84}\text{O}_2[\text{>M}(\text{C}_3\text{N}_6^+\text{C}_3)_2][\text{>M}(\text{C}_3\text{N}_6\text{C}_3)_2]-(\text{I}^-)_{10}$  (LC20)<sup>67</sup> (shown in Figs. 2(f) and (g)). Different wavelengths were used for irradiation. UVA and blue light caused more killing with LC20 than with LC19. This difference can be attributed to better chance of electron transfer process occurring with shorter wavelengths and also the presence of the electron donating tertiary-polyethyleneamine chain. While when white light was employed the variation between LC20 and LC19 was smaller but LC20 still gave extra killing, while green light gave equivalent killing for the two fullerenes. The situation was upturned and LC19 gave considerably more killing than LC20 when red light was used. It is important to state that the compounds used here induced a very low dark toxicity.

### ***In Vivo* Photodynamic Therapy of Cancer**

The three prerequisites for the fullerene PS to have photodynamic effect on tumors are first of all it should accumulate in the tumor tissue; secondly there should be a practically efficient way to administer the compound to tumor bearing animals; and thirdly a practical way to deliver excitation light to the tumors.<sup>100</sup> The first challenge in this direction was taken up by Tabata<sup>56</sup> in 1997. To make the water-insoluble pristine  $C_{60}$  water soluble and enlarge its molecular size they chemically modified it with polyethylene glycol. This conjugate was injected intravenously into mice carrying a subcutaneous tumor on the back.  $C_{60}$ -PEG conjugate demonstrated higher accumulation and relatively more prolonged retention in the tumor tissue than in normal tissue. On performing PDT after intravenous injection of  $C_{60}$ -PEG conjugate or Photofrin to tumor-bearing mice, coupled with exposure of the tumor site to visible light, the volume increase of the tumor mass was suppressed and the  $C_{60}$ -PEG conjugate exhibited a stronger suppressive effect than Photofrin. Tumor necrosis was observed without any damage to the overlying normal skin. The antitumor effect of the conjugate showed an increase with increasing fluence delivered and  $C_{60}$  dose, and cures were achieved by treatment with a low dose of 424  $\mu\text{g}/\text{kg}$  at a fluence of 107  $\text{J}/\text{cm}^2$ . In another study Liu and others<sup>55</sup> conjugated polyethylene glycol (PEG) to  $C_{60}$  ( $C_{60}$ -PEG), and diethylenetriaminepentaacetic acid (DTPA) was subsequently introduced to the terminal group of PEG to prepare  $C_{60}$ -PEG-DTPA that was mixed with gadolinium acetate solution to obtain  $\text{Gd}^{3+}$ -chelated  $C_{60}$ -PEG-DTPA-Gd. PDT induced anti-tumor effect and MRI tumor imaging was evaluated on intravenous injection of  $C_{60}$ -PEG-DTPA-Gd into the tumor bearing mice. Equivalent generation of superoxide upon illumination was observed with or without  $\text{Gd}^{3+}$  chelation. Intravenous injection of  $C_{60}$ -PEG-DTPA-Gd into tumor bearing mice plus light (400~500 nm, 53.5  $\text{J}/\text{cm}^2$ ) demonstrated significant anti-tumor PDT

depending on the timing of light irradiation that also correlated with tumor accumulation as detected by the enhanced MRI signal.

Yu and her coworkers<sup>101</sup> performed a preliminary *in vivo* study of PDT using hydrophilic nanospheres formed from hexa(sulfo-*n*-butyl)-C<sub>60</sub>(FC<sub>4</sub>S, shown in Fig. 3(A)). This study was performed on ICR mice bearing sarcoma 180 subcutaneous tumors. No adverse effects were noted in the animals when the FC<sub>4</sub>S was administered orally. Water-soluble FC<sub>4</sub>S in PBS (5 mg/kg body weight) was given either intraperitoneally or intravenously with subsequent irradiation with an argon ion laser beam at a wavelength of 515 nm or an argon-pumped dye-laser at 633 nm. The beam was focused to a diameter of 7–8 mm with the total light dose of 100 J/cm<sup>2</sup>. Inhibition of tumor growth was found more effective using the low wavelength i.e., in case of better-absorbed 515nm laser than the 633 nm laser. *I .p.* administration method proved to be slightly better in inhibition effectiveness than the i.v. method. Conclusively data suggest that PDT with fullerenes is not only possible in animal tumor models, but can demonstrate the potential use of these compounds as PS for PDT of cancer.

We have also recently shown<sup>102</sup> the therapeutic effects of intraperitoneal PDT with fullerene and white light in a very challenging mouse model of disseminated abdominal cancer. In this study we prepared the monocationic BF4 (Fig. 2(c)) in micelles composed of Cremophor EL. Colon adenocarcinoma cell line (CT26) expressing firefly luciferase was used to allow monitoring of IP tumor burden by non-invasive bioluminescence imaging. BF4 in micelles was injected intraperitoneally (5 mg/kg) followed by white-light illumination (100 J/cm<sup>2</sup>) delivered through the peritoneal wall. This produced a statistically significant reduction in bioluminescence and besides this produced a survival advantage in mice, shown in Figure 8. A drug-light interval of 24 h was more effective than a 3 h drug-light interval showing the significance of allowing enough time for the fullerene to be taken up into the cancer cells.

As the cancer cells are known to express more glucose receptors, Otake et al. exploited this fact and synthesized group of C<sub>60</sub>-glucose conjugates which also proved to be more soluble. These conjugates demonstrated selective phototoxicity compared to fibroblast cells thus suggesting the significance of targeting glucose receptors.<sup>103</sup> The PDT effect *in vivo* was investigated in human-melanoma (COLO679)-xenograft bearing mice by injecting C<sub>60</sub>-(Glc)<sub>1</sub> (0.1 or 0.2 mg/tumor) intratumorally followed by irradiated with 10 J/cm<sup>2</sup> UVA light. The drug-light interval was 4 h. Tumor growth was suppressed better with the higher dose than the lower dose.

## ANTIMICROBIAL EFFECT OF FULLERENES

Antibiotic resistance is a worldwide problem that is spreading with remarkable speed. The injudicious and over-use of antibiotics is the most important reason leading to antibiotic resistance around the world.

The “golden age” of antimicrobial therapy began with the discovery of antibiotics around the middle of the last century.<sup>104</sup> Meanwhile many other ancient effective antibacterial treatments including photosensitizing reactions were forgotten. In the last few decades, however, the widespread use of antimicrobial agents emerges the increase of antibiotic-

resistant bacteria and other infectious microorganisms and led to predictions of untreatable infections caused by “superbugs,”<sup>105</sup> which in turn has created an ever-increasing need for new drugs.

Therefore antimicrobial PDT has become an emerging alternative strategies for destroying microorganisms especially for multi-drug resistant pathogens.<sup>106</sup> PDT produces ROS that are toxic to the target microorganisms. PDT has a broad spectrum of action, and compared to antibiotic treatment PDT does not lead to the selection of mutant resistant strains.

Currently, topical application of a PS on infected tissues and subsequent illumination seems to be the most prominent feature of antimicrobial PDT, without damaging the surrounding tissue or disturbing the residual bacterial-flora. It was well accepted that Gram-positive bacteria are more susceptible to PDT as compared to Gram-negative bacteria. This can be explained by the different structures of their cell walls.<sup>107</sup>

There are several possible mechanisms to explain the antimicrobial activity of illuminated fullerene PS: by interfering with cell wall synthesis; plasma membrane integrity; nucleic acid synthesis; ribosomal function and folate synthesis. All of these would result in disruption of the bacterial cell function and inhibit their growth.

Martin and Logsdon hypothesized that it was possible that microorganisms were susceptible to damage by to Type I ROS when compared with Type II singlet oxygen.<sup>108</sup> As mentioned before fullerenes can gain solubility<sup>63</sup> and produce more hydroxyl radicals and superoxide anion, as well as singlet oxygen through functionalization<sup>109</sup> by attaching some hydrophilic or amphiphilic functional groups.<sup>22</sup>

An ideal PS proposed for antimicrobial PDT can be judged on several criteria. These PS should have no toxicity in the dark and should selectively kill bacteria over mammalian cells. PS should be able to kill multiple classes of microorganisms at relatively low concentrations with low fluences of light. PS should ideally have high absorption around 600 nm to 800 nm and generate high triplet and singlet oxygen quantum yields.

### Antimicrobial Effects *In Vitro*

The structures, especially the charges of attached groups on fullerene influence the efficacy of PS on killing microorganisms. Our lab has shown, in a series of reported experiments that cationic fullerenes fulfill many, but not all of the aforementioned criteria. At the first time we demonstrated that the soluble functionalized fullerenes were efficient antimicrobial PS and could mediate selective photodynamic inactivation (PDI) for various classes of microbial cells over mammalian cells.<sup>75</sup> We compared the antimicrobial activity of broad-spectrum antimicrobial photodynamic activities of two series of functionalized C<sub>60</sub>; a first series with one, two, or three polar diserinol groups, and a second series with one, two, or three quarternary pyrrolidinium groups. Gram-positive bacteria (*S. aureus*) Gram-negative bacteria (*E. coli* and *P. aeruginosa*), and fungal yeast (*C. albicans*) were tested in this study. The neutral, alcohol-functionalized fullerenes had only modest activity against *S. aureus*, while the cationic pyrrolidinium-functionalized fullerene (**BF6**, Fig. 2(d)) was surprisingly effective in causing light-mediated killing of *S. aureus* at 1  $\mu$ M, and 10  $\mu$ M for *E. coli*, *C.*

*albicans* and *P. aeruginosa*. However, the pyrrolidinium- functionalized fullerenes compound **BF6** demonstrated high levels of dark toxicity against *S. aureus*, Mashino et al. showed that cationic fullerenes could inhibit the growth of *E. coli* and *S. aureus* by interfering with the respiratory chain.<sup>110, 111</sup> This data suggests that photoactivated fullerenes may have somewhat different sites of action in bacteria compared to more traditional PS such as tetrapyrroles that generate singlet oxygen. These compounds all performed significantly better than a widely used antimicrobial photosensitizer, toluidine blue O.

In agreement with previous discussion, results from Spesia et al.<sup>112</sup> indicated that a dicationic fullerene derivative was an interesting PS with potential applications in PDI of bacteria. They compared the PDI efficacy of fullerene derivatives with different numbers of cationic charges. The spectroscopic and photodynamic properties of a dicationic *N,N*-dimethyl-2-(40-*N,N,N*-trimethyl-aminophenyl) fulleropyrrolidinium iodide) ( $\text{DTC}_{60}^{2+}$ ) were compared with a non-charged *N*-methyl-2-(4'-acetamidophenyl) fulleropyrrolidine ( $\text{MAC}_{60}$ ) and a monocationic *N,N*-dimethyl-2-(4'-acetamidophenyl)fulleropyrrolidinium iodide ( $\text{DAC}_{60}^{+}$ ) in different media and in a typical Gram-negative bacterium, *E. coli*. PDI of *E. coli* cellular suspensions by dicationic fullerene exhibits a ~3.5 log decrease of cell survival after 30 min of irradiation, which represents about 99.97% of cellular inactivation.

To determine the optimal chemical structures produced by fullerene derivatization, a QSAR relationship study employed fullerene PS with a wider range of different hydrophobicities, as well as with an increased number of cationic charges.<sup>113</sup> The results indicated that increasing the number of cationic charges and lowering the hydrophobicity tended to increase the antimicrobial PDI efficacy of fullerene PS against both Gram-positive and Gram-negative bacteria. The charge increases the association of the PS with negatively charged pathogen membranes, whereas the hydrophobic character increases association with or penetration into the lipid components of the membrane, or both. Recently, Mizuno et al.<sup>82</sup> from our laboratory emphasized the importance of the number of cationic charges in influencing the efficiency of the fullerenes in antimicrobial PDI when they looked at a further series of functionalized cationic fullerenes PS. They compared PDI efficacy of a new group of synthetic fullerene derivatives that possessed either basic or quaternary amino groups as antimicrobial PS against *S. aureus* (Gram-positive), *E. coli* (Gram-negative) bacteria and *C. albicans* (fungi). QSAR derived with Log P and hydrophilic lipophilic balance parameters showed that much better correlations were obtained when 3× the number of cationic charges were subtracted from the Log P values. The most effective ones to perform antimicrobial PDT were tetracationic compound **BF21** that had more cationic charges and a lower log P. *S. aureus* was most susceptible; *E. coli* was intermediate, while *C. albicans* was the most resistant species tested.

Antimicrobial effect of two highly water-soluble decacationic fullerenes **LC14**

( $\text{C}_{60}[\text{>M}(\text{C}_3\text{N}_6^+\text{C}_3)_2]$ ) and **LC17** ( $\text{C}_{70}[\text{>M}(\text{C}_3\text{N}_6^+\text{C}_3)_2]$ ) were applied for comparison in the PDT-killing of the Gram-positive *S. aureus*.<sup>66</sup> The decacationic arms attached to these fullerenes facilitated the rapid binding to the anionic residues of bacterial cell walls. The large number of ionic groups dramatically enhanced water solubility of these compounds.

The data showed interesting differences between the photoactivity of decacationic fullerene compounds that differ only in the number of carbon atoms in the fullerene cage. For Gram-positive bacteria  $C_{60}[>M(C_3N_6^+C_3)_2]$  was better at photokilling than  $C_{70}[>M(C_3N_6^+C_3)_2]$ , while for Gram-negative bacteria and for cancer cells the opposite was the case, in that  $C_{70}[>M(C_3N_6^+C_3)_2]$  was better at photokilling than  $C_{60}[>M(C_3N_6^+C_3)_2]$ . The results of ROS ( $HO^\bullet$  or  $^1O_2$ ) generation demonstrated that  $C_{60}[>M(C_3N_6^+C_3)_2]$  produced more  $^1O_2$  while  $C_{70}[>M(C_3N_6^+C_3)_2]$  produced more  $HO^\bullet$ . This finding offers an explanation of the preferential killing of Gram-positive bacteria by LC14 and the preferential killing of Gram-negative bacteria by LC17. This finding is in agreement with our previous report that Type II ROS, i.e., singlet oxygen,  $^1O_2$ , are better at killing Gram-positive bacteria than Type I ROS, i.e., hydroxyl radicals,  $HO^\bullet$ , while the reverse is true for Gram-negative bacteria ( $HO^\bullet$  is better at killing than  $^1O_2$ ). The hypothesis is that  $^1O_2$  can diffuse more easily into porous cell walls of Gram-positive bacteria to reach sensitive sites, while the less permeable Gram-negative bacterial cell wall needs the more reactive  $HO^\bullet$  to cause real damage.<sup>114, 115</sup>

### Antimicrobial Effect *In Vivo*

The absorption spectrum of fullerenes is, in addition to substantial UV absorption, mainly in the blue and green visible wavelengths. This property actually limits the application of fullerene in clinical disorders, once the penetration of short wavelength light into tissue is relatively poor; however, fullerenes may still be useful as antimicrobial PS for the treatment of relatively superficial infections, where the light does not need to penetrate deeper than 1 mm. A fullerene-based PS (BF6) with tricationic charges provided by quaternized dimethylpyrrolidinium groups was found to be an effective against Gram-positive bacteria, Gram-negative bacteria and fungal yeast *in vitro*.<sup>75</sup> To investigate if the high degree of *in vitro* activity could translate into an *in vivo* antibacterial PDT effect, our lab<sup>81</sup> continued to test BF6 in two potentially lethal mouse models of wounds infected with two Gram-negative bacteria (*P. aeruginosa* and *P. mirabilis*), respectively. Compared to Gram-positive bacteria, many Gram-negative bacteria are much more difficult to be photo-inactivated, and tend to produce systemic sepsis after developing infections in wounds. Higher concentrations of PS and higher fluences of light ( $180 \text{ J/cm}^2$ ) were needed *in vivo* than *in vitro* to achieve a certain loss of bioluminescence. The fullerene-mediated PDT succeeded in saving the life of mice whose wounds were infected with *P. mirabilis* and could be combined with a suboptimal dose of antibiotics to save mice with *P. aeruginosa* wound infections. These exciting results shown in Figure 9 indicated that fullerene-mediated PDT could either treat wounds infected with virulent species of Gram-negative bacteria or be able to synergize with a suboptimal antibiotic regimen to prevent regrowth and produce significantly higher survival.<sup>81</sup>

In the case of the 3rd-degree burns, they are particularly susceptible to bacterial infection as the barrier function of the skin is destroyed, the dead tissue is devoid of host-defense elements, and a systemic immune suppression is a worrying consequence of serious burns. Furthermore, the lack of perfusion of the burned tissue means that systemic antibiotics are generally ineffective.<sup>116</sup> Although excision and skin grafting is now standard treatment for the 3rd-degree burns,<sup>117</sup> superimposed infection is still a major problem. Patients with

Gram-negative burn infections have a higher likelihood of developing sepsis than Gram-positive infections. Topical antimicrobials are the mainstay of therapy for burn infections and PDT may have a major role to play in the management of this disease.<sup>118</sup>

We found in previous study a decacationic fullerene LC17 ( $C_{70}[>M(C_3N_6^+C_3)_2]$ ) was effective at mediating the photokilling of Gram-negative bacteria *in vitro*.<sup>66</sup> We synthesized a new compound  $C_{70}[>M(C_3N_6^+C_3)_2][>M(C_3N_6C_3)_2]$  (LC18) with the same decacationic side chain plus an additional deca-tertiary amine groups against Gram-negative bacteria. A mouse model of the third-degree burn infection with bioluminescent Gram-negative bacteria was used to test the *in vivo* effectiveness of the therapeutic approach using the UVA excitation.<sup>119</sup> The data shown in Figures 10 and 11 suggested that the attachment of an additional deca(tertiary-ethylenylamino) malonate arm to  $C_{70}$ , producing LC18, allowed the moiety to act as a potent electron donor and increased the generation yield of hydroxyl radicals under UVA illumination. This is consistent with the reported phenomena of photoinduced intramolecular electron transfer from the tertiary amine moiety to the fullerene cage in polar solvents, including water, at the short excitation wavelength. With the availability of ten tertiary amine moieties, each capable of donating one electron to the  $C_{70}$  cage, LC18 may function as an electron-rich precursor for hydroxyl radical production that demonstrated a new approach in enhancing  $HO^\bullet$  radical killing of pathogenic bacteria in contrast to the more common  $^1O_2$ -killing mechanism.

## CONCLUSION

Fullerenes have been widely studied as potential PS that could mediate PDT of diverse diseases. As discussed previously fullerene-derivatives have uniquely important favorable properties and an unusual photochemical mechanism, which could make them candidates for ideal PS. As shown by us and by others, fullerene-derivatives produce a substantial amount of superoxide anion in a Type I photochemical process involving electron transfer from the excited triplet state to molecular oxygen in aqueous biomedical solutions. It is assumed that hydroxyl radicals are formed from hydrogen peroxide, and hydroxyl radicals are the most reactive and potentially the most cytotoxic of all ROS.

The chief disadvantage of fullerenes is likely to be that their absorption spectrum of fullerenes is highest in the UVA and blue regions of the spectrum, which limit the tissue penetration depth of illumination. With the correct functionalities present on the fullerene cage, these difficulties may be overcome. Since *in vivo* PDT usually uses red light for its improved tissue-penetrating properties it is unclear whether fullerenes would mediate effective PDT *in vivo*. Therefore synthesis of new fullerene derivatives will be a trend for future study, particularly those with light-harvesting antennae to broaden the absorption light, hence increasing light penetration depth into tissue. Furthermore 2-photon excitation is another promising avenue to increase penetration depth of PDT. The mechanistic study of Type I and Type II photochemistry, and the correlations between fullerene structure, photochemical mechanism and PDT efficacy will establish whether fullerenes can compete with more traditional PS in clinical applications of PDT.

## Acknowledgments

Long Y. Chiang was supported by US NIH grant R01CA137108. Michael R. Hamblin was supported by US NIH grant R01AI050875.

## References

1. Henderson BW, Dougherty TJ. How does photodynamic therapy work? *Photochem Photobiol.* 1992; 55:145. [PubMed: 1603846]
2. Agostinis P, Berg K, Cengel KA, Foster TH, Girotti AW, Gollnick SO, Hahn SM, Hamblin MR, Juzeniene A, Kessel D, Korbelik M, Moan J, Mroz P, Nowis D, Piette J, Wilson BC, Golab J. Photodynamic therapy of cancer: An update. *CA Cancer J Clin.* 2011; 61:250. [PubMed: 21617154]
3. Boyle RW, Dolphin D. Structure and biodistribution relationships of photodynamic sensitizers. *Photochem Photobiol.* 1996; 64:469. [PubMed: 8806226]
4. Sternberg ED, Dolphin D, Brückner C. Porphyrin-based photosensitizers for use in photodynamic therapy. *Tetrahedron.* 1998; 54:4151.
5. Ravindra, K.; Pandey, RK.; Zheng, G. Porphyrins as photosensitizers in photodynamic therapy, *The Porphyrin Handbook*. Kadish, K.; Guillard, R.; Smiths, KM., editors. Vol. 6. Elsevier; San Diego: 2000. p. 157-161.
6. Allison RR, Downie GH, Cuenca R, Hu XH, Childs CJ, Sibata CH. Photosensitizers in clinical PDT. *Photodiagnosis Photodyn Ther.* 2004; 1:27. [PubMed: 25048062]
7. Weersink RA, Bogaards A, Gertner M, Davidson SR, Zhang K, Netchev G, Trachtenberg J, Wilson BC. Techniques for delivery and monitoring of TOOKAD (WST09)-mediated photodynamic therapy of the prostate: Clinical experience and practicalities. *J Photochem Photobiol B: Biol.* 2005; 79:211.
8. Hopper C, Niziol C, Sidhu M. The cost-effectiveness of Foscan mediated photodynamic therapy (Foscan-PDT) compared with extensive palliative surgery and palliative chemotherapy for patients with advanced head and neck cancer in the UK. *Oral Oncol.* 2004; 40:372. [PubMed: 14969816]
9. Krammer B, Plaetzer K. ALA and its clinical impact, from bench to bedside. *Photochem Photobiol Sci.* 2008; 7:283. [PubMed: 18389144]
10. Allen CM, Sharman WM, Van Lier JE. Current status of phthalocyanines in the photodynamic therapy of cancer. *J Porphyrins Phthalocyanines.* 2001; 5:161.
11. St Denis TG, Hamblin MR. Synthesis, bioanalysis and biodistribution of photosensitizer conjugates for photodynamic therapy. *Bioanalysis.* 2013; 5:1099. [PubMed: 23641699]
12. Leonard KA, Nelen MI, Simard TP, Davies SR, Gollnick SO, Oseroff AR, Gibson SL, Hilf R, Chen LB, Detty MR. Synthesis and evaluation of chalcogenopyrylium dyes as potential sensitizers for the photodynamic therapy of cancer. *J Med Chem.* 1999; 42:3953. [PubMed: 10508443]
13. Harris F, Chatfield LK, Phoenix DA. Phenothiazinium based photosensitizers—photodynamic agents with a multiplicity of cellular targets and clinical applications. *Curr Drug Targets.* 2005; 6:615. [PubMed: 16026282]
14. Lin CW, Shulok JR, Wong YK, Schanbacher CF, Cincotta L, Foley JW. Photosensitization, uptake, and retention of phenoxazine Nile blue derivatives in human bladder carcinoma cells. *Cancer Res.* 1991; 51:1109. [PubMed: 1847656]
15. Olivo M, Chin W. Perylenequinones in photodynamic therapy: Cellular versus vascular response. *J Environ Pathol Toxicol Oncol.* 2006; 25:223. [PubMed: 16566720]
16. Kamkaew A, Lim SH, Lee HB, Kiew LV, Chung LY, Burgess K. BODIPY dyes in photodynamic therapy. *Chem Soc Rev.* 2013; 42:77. [PubMed: 23014776]
17. Avirah RR, Jayaram DT, Adarsh N, Ramaiah D. Squaraine dyes in PDT: From basic design to *in vivo* demonstration. *Org Biomol Chem.* 2012; 10:911. [PubMed: 22179414]
18. Kavarnos GJ, Turro NJ. Photosensitization by reversible electron transfer: Theories, experimental evidence, and examples. *Chem Rev.* 1986; 86:401.
19. Accorsi G, Armaroli N. Taking advantage of the electronic excited states of [60]-fullerenes. *J Phys Chem C.* 2010; 114:1385.

20. Mroz P, Pawlak A, Satti M, Lee H, Wharton T, Gali H, Sarna T, Hamblin MR. Functionalized fullerenes mediate photodynamic killing of cancer cells: Type I versus Type II photochemical mechanism. *Free Radic Biol Med.* 2007; 43:711. [PubMed: 17664135]
21. Wang M, Nalla V, Jeon S, Mamidala V, Ji W, Tan LS, Cooper T, Chiang LY. Large femtosecond two-photon absorption cross sections of fullerosome vesicle nanostructures derived from a highly photoresponsive amphiphilic C60-light-harvesting fluorene dyad. *J Phys Chem C.* 2011; 115:18552.
22. Culotta L, Koshland DE Jr. Buckyballs: Wide open playing field for chemists. *Science.* 1991; 254:1706. [PubMed: 17829222]
23. Meng J, Wang DL, Wang PC, Jia L, Chen C, Liang XJ. Biomedical activities of endohedral metallofullerene optimized for nanopharmaceuticals. *J Nanosci Nanotechnol.* 2010; 10:8610. [PubMed: 21121373]
24. Brant JA, Labille J, Robichaud CO, Wiesner M. Fullerol cluster formation in aqueous solutions: Implications for environmental release. *J Colloid Interface Sci.* 2007; 314:281. [PubMed: 17583721]
25. Angelini G, De Maria P, Fontana A, Pierini M, Maggini M, Gasparrini F, Zappia G. Study of the aggregation properties of a novel amphiphilic C60 fullerene derivative. *Langmuir.* 2001; 17:6404.
26. Baffreau J, Leroy-Lhez S, Vân Anh N, Williams RM, Hudhomme P. Fullerene C60–Perylene-3, 4:9, 10-bis (dicarboximide) light-harvesting dyads: Spacer-length and bay-substituent effects on intramolecular singlet and triplet energy transfer. *Chem Eur J.* 2008; 14:4974. [PubMed: 18418841]
27. Tuchin VV, Wang RK, Yeh AT. Optical clearing of tissues and cells. *J Biomed Opt.* 2008; 13:021101. [PubMed: 18465950]
28. Hirshburg J, Choi B, Nelson JS, Yeh AT. Correlation between collagen solubility and skin optical clearing using sugars. *Lasers Surg Med.* 2007; 39:140. [PubMed: 17311267]
29. Jiang J, Boese M, Turner P, Wang RK. Penetration kinetics of dimethyl sulphoxide and glycerol in dynamic optical clearing of porcine skin tissue *in vitro* studied by Fourier transform infrared spectroscopic imaging. *J Biomed Opt.* 2008; 13:021105. [PubMed: 18465954]
30. Kogan A, Garti N. Microemulsions as transdermal drug delivery vehicles. *Adv Colloid Interface Sci.* 2006; 123–126:369.
31. Bhawalkar JD, Kumar ND, Zhao CF, Prasad PN. Two-photon photodynamic therapy. *J Clin Laser Med Surg.* 1997; 15:201. [PubMed: 9612170]
32. Karotki A, Khurana M, Lepock JR, Wilson BC. Simultaneous two-photon excitation of photofrin in relation to photodynamic therapy. *Photochem Photobiol.* 2006; 82:443. [PubMed: 16613497]
33. Samkoe KS, Clancy AA, Karotki A, Wilson BC, Cramb DT. Complete blood vessel occlusion in the chick chorioallantoic membrane using two-photon excitation photodynamic therapy: Implications for treatment of wet age-related macular degeneration. *J Biomed Opt.* 2007; 12:034025. [PubMed: 17614733]
34. Samkoe KS, Cramb DT. Application of an *ex ovo* chicken chorioallantoic membrane model for two-photon excitation photodynamic therapy of age-related macular degeneration. *J Biomed Opt.* 2003; 8:410. [PubMed: 12880346]
35. Oberdorster G. Safety assessment for nanotechnology and nanomedicine: Concepts of nanotoxicology. *J Intern Med.* 2010; 267:89. [PubMed: 20059646]
36. Arbogast JW, Darmany AP, Foote CS, Diederich FN, Whetten R, Rubin Y, Alvarez MM, Anz SJ. Photophysical properties of sixty atom carbon molecule (C60). *J Phys Chem A.* 1991; 95:11.
37. Haddon R, Brus LE, Raghavachari K. Electronic structure and bonding in icosahedral C60. *Chem Phys Lett.* 1986; 125:459.
38. Wu W, Zhao J, Sun J, Guo S. Light-harvesting fullerene dyads as organic triplet photosensitizers for triplet–triplet annihilation upconversions. *J Org Chem.* 2012; 77:5305. [PubMed: 22616881]
39. Yamakoshi Y, Umezawa N, Ryu A, Arakane K, Miyata N, Goda Y, Masumizu T, Nagano T. Active oxygen species generated from photoexcited fullerene (C60) as potential medicines: O<sub>2</sub><sup>•-</sup> versus <sup>1</sup>O<sub>2</sub>. *J Am Chem Soc.* 2003; 125:12803. [PubMed: 14558828]
40. Xie Q, Perez-Cordero E, Echegoyen L. Electrochemical detection of C60- and C70-: Enhanced stability of fullerides in solution. *J Am Chem Soc.* 1992; 114:3978.

41. Guldi DM, Prato M. Excited-state properties of C(60) fullerene derivatives. *Acc Chem Res.* 2000; 33:695. [PubMed: 11041834]
42. Ohkubo K, Kitaguchi H, Fukuzumi S. Activation of electron-transfer reduction of oxygen by hydrogen bond formation of superoxide anion with ammonium ion. *J Phys Chem A.* 2006; 110:11613. [PubMed: 17034154]
43. Andrievsky GV, Bruskov VI, Tykhomyrov AA, Gudkov SV. Peculiarities of the antioxidant and radioprotective effects of hydrated C60 fullerene nanostructures *in vitro* and *in vivo*. *Free Radic Biol Med.* 2009; 47:786. [PubMed: 19539750]
44. Avdeev MV, Khokhryakov AA, Tropin TV, Andrievsky GV, Klochkov VK, Derevyanchenko LI, Rosta L, Garamus VM, Priezzhev VB, Korobov MV, Aksenov VL. Structural features of molecular-colloidal solutions of C60 fullerenes in water by small-angle neutron scattering. *Langmuir.* 2004; 20:4363. [PubMed: 15969139]
45. de La Vaissière B, Sandall JP, Fowler PW, de Oliveira P, Bensasson RV. Regioselectivity in radical reactions of C60 derivatives. *J Chem Soc Perkin.* 2001; 2:821.
46. Gharbi N, Pressac M, Hadchouel M, Szwarc H, Wilson SR, Moussa F. [60]fullerene is a powerful antioxidant *in vivo* with no acute or subacute toxicity. *Nano Lett.* 2005; 5:2578. [PubMed: 16351219]
47. Kato S, Aoshima H, Saitoh Y, Miwa N. Fullerene-C60/liposome complex: Defensive effects against UVA-induced damages in skin structure, nucleus and collagen type I/IV fibrils, and the permeability into human skin tissue. *J Photochem Photobiol B.* 2010; 98:99. [PubMed: 20036139]
48. Doi Y, Ikeda A, Akiyama M, Nagano M, Shigematsu T, Ogawa T, Takeya T, Nagasaki T. Intracellular uptake and photodynamic activity of water-soluble [60]- and [70]fullerenes incorporated in liposomes. *Chemistry.* 2008; 14:8892. [PubMed: 18698574]
49. Yan A, Von Dem Bussche A, Kane AB, Hurt RH. Tocopheryl polyethylene glycol succinate as a safe, antioxidant surfactant for processing carbon nanotubes and fullerenes. *Carbon N Y.* 2007; 45:2463. [PubMed: 19081834]
50. Akiyama M, Ikeda A, Shintani T, Doi Y, Kikuchi J, Ogawa T, Yogo K, Takeya T, Yamamoto N. Solubilisation of [60]fullerenes using block copolymers and evaluation of their photodynamic activities. *Org Biomol Chem.* 2008; 6:1015. [PubMed: 18327326]
51. Kojima C, Toi Y, Harada A, Kono K. Aqueous solubilization of fullerenes using poly(amidoamine) dendrimers bearing cyclodextrin and poly(ethylene glycol). *Bioconjug Chem.* 2008; 19:2280. [PubMed: 18844391]
52. Pan B, Cui D, Xu P, Ozkan C, Feng G, Ozkan M, Huang T, Chu B, Li Q, He R, Hu G. Synthesis and characterization of polyamidoamine dendrimer-coated multi-walled carbon nanotubes and their application in gene delivery systems. *Nanotechnology.* 2009; 20:125101. [PubMed: 19420458]
53. Hooper JB, Bedrov D, Smith GD. Supramolecular self-organization in PEO-modified C60 fullerene/water solutions: Influence of polymer molecular weight and nanoparticle concentration. *Langmuir.* 2008; 24:4550. [PubMed: 18402490]
54. Nitta N, Seko A, Sonoda A, Ohta S, Tanaka T, Takahashi M, Murata K, Takemura S, Sakamoto T, Tabata Y. Is the use of fullerene in photodynamic therapy effective for atherosclerosis? *Cardiovasc Intervent Radiol.* 2008; 31:359. [PubMed: 18040738]
55. Liu J, Ohta S, Sonoda A, Yamada M, Yamamoto M, Nitta N, Murata K, Tabata Y. Preparation of PEG-conjugated fullerene containing Gd<sup>3+</sup> ions for photodynamic therapy. *J Control Release.* 2007; 117:104. [PubMed: 17156882]
56. Tabata Y, Murakami Y, Ikada Y. Photodynamic effect of polyethylene glycol-modified fullerene on tumor. *Jpn J Cancer Res.* 1997; 88:1108. [PubMed: 9439687]
57. Bali V, Ali M, Ali J. Novel nanoemulsion for minimizing variations in bioavailability of ezetimibe. *J Drug Target.* 2010; 18:506. [PubMed: 20067438]
58. Amani A, York P, Chrystyn H, Clark BJ. Factors affecting the stability of nanoemulsions—use of artificial neural networks. *Pharm Res.* 2010; 27:37. [PubMed: 19908130]
59. Bansal T, Mustafa G, Khan ZI, Ahmad FJ, Khar RK, Talegaonkar S. Solid self-nanoemulsifying delivery systems as a platform technology for formulation of poorly soluble drugs. *Crit Rev Ther Drug Carrier Syst.* 2008; 25:63. [PubMed: 18540836]

60. Shakeel F, Faisal MS. Nanoemulsion: A promising tool for solubility and dissolution enhancement of celecoxib. *Pharm Dev Technol.* 2010; 15:53. [PubMed: 19552546]
61. Filippone S, Heimann F, Rassat A. A highly water-soluble 2:1 beta-cyclodextrin-fullerene conjugate. *Chem Commun (Camb).* 2002;1508. [PubMed: 12189867]
62. Zhao B, He YY, Bilski PJ, Chignell CF. Pristine (C60) and hydroxylated [C60(OH)24] fullerene phototoxicity towards HaCaT keratinocytes: Type I versus type II mechanisms. *Chem Res Toxicol.* 2008; 21:1056. [PubMed: 18422350]
63. Nakamura E, Isobe H. Functionalized fullerenes in water. The first 10 years of their chemistry, biology, and nanoscience. *Acc Chem Res.* 2003; 36:807. [PubMed: 14622027]
64. Yurovskaya MA, Trushkov IV. Cycloaddition to buckmin-sterfullerene C60: Advancements and future prospects. *Russ Chem Bull.* 2002; 51:367.
65. Maggini M, Scorrano G, Prato M. Addition of azomethine ylides to C60: Synthesis, characterization, and functionalization of fullerene pyrrolidines. *J Am Chem Soc.* 1993; 115:9798.
66. Wang M, Huang L, Sharma SK, Jeon S, Thota S, Sperandio FF, Nayka S, Chang J, Hamblin MR, Chiang LY. Synthesis and photodynamic effect of new highly photostable decacationically armed [60]- and [70]fullerene decaiodide monoadducts to target pathogenic bacteria and cancer cells. *J Med Chem.* 2012; 55:4274. [PubMed: 22512669]
67. Sperandio FF, Sharma SK, Wang M, Jeon S, Huang YY, Dai T, Nayka S, de Sousa SC, Chiang LY, Hamblin MR. Photoinduced electron-transfer mechanisms for radical-enhanced photodynamic therapy mediated by water-soluble decacationic C70 and C84O2 Fullerene Derivatives. *Nanomedicine.* 2013; 9:570. [PubMed: 23117043]
68. Brettreich M, Burghardt S, Bottcher C, Bayerl T, Bayerl S, Hirsch A. Globular amphiphiles: Membrane-forming hexaadducts of C(60). *Angew Chem Int Ed Engl.* 2000; 39:1845. [PubMed: 10934382]
69. Tegos GP, Demidova TN, Arcila-Lopez D, Lee H, Wharton T, Gali H, Hamblin MR. Cationic fullerenes are effective and selective antimicrobial photosensitizers. *Chem Biol.* 2005; 12:1127. [PubMed: 16242655]
70. Wang M, Maragani S, Huang L, Jeon S, Canteenwala T, Hamblin MR, Chiang LY. Synthesis of decacationic [60]fullerene decaiodides giving photoinduced production of superoxide radicals and effective PDT-mediation on antimicrobial photoinactivation. *Eur J Med Chem.* 2013; 63:170. [PubMed: 23474903]
71. Thota S, Wang M, Jeon S, Maragani S, Hamblin MR, Chiang LY. Synthesis and characterization of positively charged pentacationic [60]fullerene monoadducts for antimicrobial photodynamic inactivation. *Molecules.* 2012; 17:5225. [PubMed: 22565476]
72. Constantin C, Neagu M, Ion RM, Gherghiceanu M, Stavaru C. Fullerene-porphyrin nanostructures in photodynamic therapy. *Nanomedicine (Lond).* 2010; 5:307. [PubMed: 20148640]
73. Chiang LY, Padmawar PA, Rogers-Haley JE, So G, Canteenwala T, Thota S, Tan LS, Pritzker K, Huang YY, Sharma SK, Kurup DB, Hamblin MR, Wilson B, Urbas A. Synthesis and characterization of highly photoresponsive fullereryl dyads with a close chromophore antenna-C(60) contact and effective photodynamic potential. *J Mater Chem.* 2010; 20:5280. [PubMed: 20890406]
74. El-Khouly ME, Padmawar P, Araki Y, Verma S, Chiang LY, Ito O. Photoinduced processes in a tricomponent molecule consisting of diphenylaminofluorene-dicyanoethylenemethano[60]fullerene. *J Phys Chem A.* 2006; 110:884. [PubMed: 16419985]
75. Tegos GP, Demidova TN, Arcila-Lopez D, Lee H, Wharton T, Gali H, Hamblin MR. Cationic fullerenes are effective and selective antimicrobial photosensitizers. *Chem Biol.* 2005; 12:1127. [PubMed: 16242655]
76. Diederich F, Gómez-López M. Supramolecular fullerene chemistry. *Chem Soc Rev.* 1999; 28:263.
77. Kadish, KM.; Ruoff, RS., editors. Fullerenes: Chemistry, Physics, and Technology. John Wiley & Sons Inc; New York: 2000.
78. Hu Z, Guan W, Wang W, Huang L, Xing H, Zhu Z. Protective effect of a novel cystine C(60) derivative on hydrogen peroxide-induced apoptosis in rat pheochromocytoma PC12 cells. *Chem Biol Interact.* 2007; 167:135. [PubMed: 17353010]
79. Bingel C. ChemInform abstract: Cyclopropylation of fullerenes. *ChemInform.* 1994; 25:1957.

80. Maggini M, Scorrano G, Prato M. Addition of azomethine ylides to C<sub>60</sub>-synthesis, characterization, and functionalization of fullerenes pyrrolidines. *J Am Chem Soc.* 1993; 115:9798.
81. Lu Z, Dai T, Huang L, Kurup DB, Tegos GP, Jahnke A, Wharton T, Hamblin MR. Photodynamic therapy with a cationic functionalized fullerene rescues mice from fatal wound infections. *Nanomedicine (Lond).* 2010; 5:1525. [PubMed: 21143031]
82. Mizuno K, Zhiyentayev T, Huang L, Khalil S, Nasim F, Tegos GP, Gali H, Jahnke A, Wharton T, Hamblin MR. Antimicrobial photodynamic therapy with functionalized fullerenes: Quantitative structure-activity relationships. *J Nanomed Nanotechnol.* 2011; 2:1. [PubMed: 21743839]
83. Wang M, Huang L, Sharma SK, Jeon S, Thota S, Sperandio FF, Nayka SN, Chang J, Hamblin MR, Chiang LY. Synthesis and photodynamic effect of new highly photostable decacationically armed [60]-and [70] fullerene decaiodide monoadducts to target pathogenic bacteria and cancer cells. *J Med Chem.* 2012; 55:4274. [PubMed: 22512669]
84. Bhonsle JB, Chi Y, Huang JP, Shiea J, Chen BJ, Chiang LY. Novel water-soluble hexa(sulfobutyl)fullerenes as potent free radical scavengers. *Chem Lett.* 1998; 27:465.
85. Yu C, Canteenwala T, El-Khouly ME, Araki Y, Pritzker K, Ito O, Wilson BC, Chiang LY. Efficiency of singlet oxygen production from self-assembled nanospheres of molecular micelle-like photosensitizers FC4S. *J Mater Chem.* 2005; 15:857.
86. Jeng US, Lin TL, Tsao CS, LCH, Canteenwala T, Wang LY, Chiang LY, Han CC. Study of aggregates of fullerene-based ionomers in aqueous solutions using small angle neutron and X-ray scattering. *J Phys Chem B.* 1999; 103:1059.
87. Guldi DM, Asmus KD. Photophysical properties of mono- and multiply-functionalized fullerene derivatives. *J Phys Chem B.* 1997; 101:1472.
88. Bensasson RV, Berberan-Santos MN, Bretreick M, Frederiksen J, Göttinger H, Hirsch A, Land EJ, Leach S, McGarvey DJ, Schönberger H, Schröder C. Triplet state properties of malonic acid C<sub>60</sub> derivatives C<sub>60</sub>[C(COOR)<sub>2</sub>]<sub>n</sub>; R H, Et; n = 1–6. *Phys Chem Chem Phys.* 2001; 3:4679.
89. Foley S, Crowley C, Smaih M, Bonfils C, Erlanger BF, Seta P, Larroque C. Cellular localisation of a water-soluble fullerene derivative. *Biochem Biophys Res Commun.* 2002; 294:116. [PubMed: 12054749]
90. Porter AE, Gass M, Muller K, Skepper JN, Midgley P, Welland M. Visualizing the uptake of C<sub>60</sub> to the cytoplasm and nucleus of human monocyte-derived macrophage cells using energy-filtered transmission electron microscopy and electron tomography. *Environ Sci Technol.* 2007; 41:3012. [PubMed: 17533872]
91. Tokuyama H, Yamago S, Nakamura E, Shiraki T, Sugiura Y. Photoinduced biochemical activity of fullerene carboxylic acid. *J Am Chem Soc.* 1993; 115:7918.
92. Burlaka AP, Sidorik YP, Prylutska SV, Matyshevska OP, Golub OA, Prylutsky YI, Scharff P. Catalytic system of the reactive oxygen species on the C<sub>60</sub> fullerene basis. *Exp Oncol.* 2004; 26:326. [PubMed: 15627068]
93. Rancan F, Rosan S, Boehm F, Cantrell A, Brellreich M, Schoenberger H, Hirsch A, Moussa F. Cytotoxicity and photocytotoxicity of a dendritic C(60) mono-adduct and a malonic acid C(60) tris-adduct on Jurkat cells. *J Photochem Photobiol B.* 2002; 67:157. [PubMed: 12167314]
94. Rancan F, Helmreich M, Molich A, Jux N, Hirsch A, Roder B, Witt C, Bohm F. Fullerene-pyropheophorbide a complexes as sensitizer for photodynamic therapy: Uptake and photo-induced cytotoxicity on Jurkat cells. *J Photochem Photobiol B.* 2005; 80:1. [PubMed: 15963432]
95. Li R, Bounds DJ, Granville D, Ip SH, Jiang H, Margaron P, Hunt DW. Rapid induction of apoptosis in human keratinocytes with the photosensitizer QLT0074 via a direct mitochondrial action. *Apoptosis.* 2003; 8:269. [PubMed: 12766487]
96. Gupta S, Ahmad N, Mukhtar H. Involvement of nitric oxide during phthalocyanine (Pc4) photodynamic therapy-mediated apoptosis. *Cancer Res.* 1998; 58:1785. [PubMed: 9581812]
97. Elisa Milanesio M, Alvarez MG, Rivarola V, Silber JJ, Durantini EN. Porphyrin-fullerene C<sub>60</sub> dyads with high ability to form photoinduced charge-separated state as novel sensitizers for photodynamic therapy. *Photochem Photobiol.* 2005; 81:891. [PubMed: 15757366]

98. Alvarez MG, Prucca C, Milanesio ME, Durantini EN, Rivarola V. Photodynamic activity of a new sensitizer derived from porphyrin-C60 dyad and its biological consequences in a human carcinoma cell line. *Int J Biochem Cell Biol.* 2006; 38:2092. [PubMed: 16899389]
99. Elisa Milanesio M, Gabriela Alvarez M, Durantini EN. Methoxyphenyl porphyrin derivatives as phototherapeutic agents. *Curr Bioact Compd.* 2010; 6:97.
100. Mroz P, Tegos GP, Gali H, Wharton T, Sarna T, Hamblin MR. Photodynamic therapy with fullerenes. *Photochem Photobiol Sci.* 2007; 6:1139. [PubMed: 17973044]
101. Yu, C.; Canteenwala, T.; Chen, HH.; Jeng, U-S.; Lin, T-L.; Chiang, LY. Free radical scavenging and photodynamic functions of micelle-like hydrophilic hexa (sulfobutyl) fullerene (FC4S). In: sawas, E., editor. *Perspectives of Fullerene Nanotechnology.* Springer; Netherlands: 2002. p. 165-183.
102. Mroz P, Xia Y, Asanuma D, Konopko A, Zhiyentayev T, Huang YY, Sharma SK, Dai T, Khan UJ, Wharton T, Hamblin MR. Intraperitoneal photodynamic therapy mediated by a fullerene in a mouse model of abdominal dissemination of colon adenocarcinoma. *Nanomedicine.* 2011; 7:965. [PubMed: 21645643]
103. Otake E, Sakuma S, Torii K, Maeda A, Ohi H, Yano S, Morita A. Effect and mechanism of a new photodynamic therapy with glycoconjugated fullerene. *Photochem Photobiol.* 2010; 86:1356. [PubMed: 20796243]
104. Maisch T. A new strategy to destroy antibiotic resistant microorganisms: Antimicrobial photodynamic treatment. *Mini Rev Med Chem.* 2009; 9:974. [PubMed: 19601890]
105. Talan DA. MRSA: Deadly super bug or just another staph? *Ann Emerg Med.* 2008; 51:299. [PubMed: 18222565]
106. Hamblin MR, Hasan T. Photodynamic therapy: A new antimicrobial approach to infectious disease? *Photochem Photobiol Sci.* 2004; 3:436. [PubMed: 15122361]
107. Hancock RE, Bell A. Antibiotic uptake into gram-negative bacteria. *Eur J Clin Microbiol Infect Dis.* 1988; 7:713. [PubMed: 2850910]
108. Martin JP, Logsdon N. The role of oxygen radicals in dye-mediated photodynamic effects in *Escherichia coli* B. *J Biol Chem.* 1987; 262:7213. [PubMed: 3034885]
109. Duncan LK, Jinschek JR, Vikesland PJ. C<sub>60</sub> colloid formation in aqueous systems: Effects of preparation method on size, structure, and surface charge. *Environ Sci Technol.* 2008; 42:173. [PubMed: 18350893]
110. Mashino T, Usui N, Okuda K, Hirota T, Mochizuki M. Respiratory chain inhibition by fullerene derivatives: Hydrogen peroxide production caused by fullerene derivatives and a respiratory chain system. *Bioorg Med Chem.* 2003; 11:1433. [PubMed: 12628669]
111. Mashino T, Okuda K, Hirota T, Hirobe M, Nagano T, Mochizuki M. Inhibition of *E. coli* growth by fullerene derivatives and inhibition mechanism. *Bioorg Med Chem Lett.* 1999; 9:2959. [PubMed: 10571155]
112. Spesia MB, Milanesio ME, Durantini EN. Synthesis, properties and photodynamic inactivation of *Escherichia coli* by novel cationic fullerene C<sub>60</sub> derivatives. *Eur J Med Chem.* 2008; 43:853. [PubMed: 17706838]
113. Dai T, Huang YY, Sharma SK, Hashmi JT, Kurup DB, Hamblin MR. Topical antimicrobials for burn wound infections. *Recent Pat Antiinfect Drug Discov.* 2010; 5:124. [PubMed: 20429870]
114. Dahl TA, Midden WR, Hartman PE. Comparison of killing of gram-negative and gram-positive bacteria by pure singlet oxygen. *J Bacteriol.* 1989; 171:2188–2194. [PubMed: 2703469]
115. Valduga G, Bertoloni G, Reddi E, Jori G. Effect of extracellularly generated singlet oxygen on gram-positive and gram-negative bacteria. *J Photochem Photobiol B.* 1993; 21:81. [PubMed: 8289115]
116. Ollstein RN, McDonald C. Topical and systemic antimicrobial agents in burns. *Ann Plast Surg.* 1980; 5:386. [PubMed: 6779699]
117. Saffle JR. Closure of the excised burn wound: Temporary skin substitutes. *Clin Plast Surg.* 2009; 36:627. [PubMed: 19793557]
118. Dai T, Huang YY, Sharma SK, Hashmi JT, Kurup DB, Hamblin MR. Topical antimicrobials for burn wound infections. *Recent Pat Antiinfect Drug Discov.* 2010; 5:124. [PubMed: 20429870]

119. Huang L, Wang M, Dai T, Sperandio FF, Huang YY, Xuan Y, Chiang LY, Hamblin MR. Antimicrobial photodynamic therapy with decacationic monoadducts and bisadducts of [70]fullerene: *In vitro* and *in vivo* studies. *Nanomedicine (Lond)*. 2013; 9:253. [PubMed: 23738632]

## Biographies



**Ying-Ying Huang, M.D.**, is a researcher in Dr. Michael Hamblin's lab in Wellman Center for Photomedicine at Massachusetts General Hospital, an Instructor of Dermatology at Harvard Medical School. She received her M.D. from China in 2004. She earned her M.Med in Dermatology in China and she was trained as a dermatologist. She has been at MGH Wellman Center for 5 years. Her research interests lie in the areas of photodynamic therapy (PDT) for infections, cancer and mechanism of low level light therapy (LLLT) for traumatic brain injury. She has published 48 peer review articles and 15 conference proceedings and book chapters. She is the co-editor of newly released "Handbook of Photomedicine."



**Sulbha K. Sharma, Ph.D.** is a visiting fellow at Raja Ramanna centre for advanced technology, Indore, India. Earlier she was a postdoctoral fellow at Dr. Hamblin's lab at The Wellman Center for Photomedicine, Massachusetts General Hospital, Boston, MA. She completed her Ph.D. from Laser Biomedical section and instrumentation division at Raja Ramanna centre for advanced technology, Indore, India. She has published 25 peer-reviewed articles 7 conference proceedings and 4 book chapters. Her research interests are anticancer photodynamic therapy and low level light therapy.



**Rui Yin, M.D., Ph.D.** is an Associate Professor of Dermatology, Southwest Hospital, Third Military Medical University, and a visiting associate professor of Wellman Center for

Photomedicine at Massachusetts General Hospital. Her research interests lie in the areas of photodynamic therapy for infections and cancer, the electron transfer mechanisms of photodynamic reaction. She has published 17 peer-reviewed articles in English, over 40 peer-reviewed articles in Chinese, over 30 conference proceeding, 2 book chapters. She is a reviewer for 7 journals and serves on National Natural Science Foundation of China as a grant reviewer. She is also a committee member of China Dermatologist Association and China Medical Association. In 2011, Dr. Yin was honored as one of Top 10 National Outstanding Young Dermatologist by China Dermatologist Association.



**Tanupriya Agrawal**, M.D., Ph.D. is a postdoctoral fellow at Dr. Hamblin's lab at The Wellman Center for Photomedicine, Massachusetts General Hospital, Boston, MA. Prior to this, she finished medical school at N.S.C.B Medical College, Jabalpur, India followed by Ph.D. in Biomedical Sciences at Creighton University, Omaha, NE. She has completed United States Medical Licensing Examination (USMLE) and certified by Educational Commission for Foreign Medical Graduates (ECFMG). She has published 6 peer-reviewed articles and 12 conference proceedings. She is investigating the role and underlying molecular mechanisms of low level laser therapy in neurogenesis and synaptogenesis in mouse model of traumatic brain injury.



**Long Y. Chiang**, Ph.D. is a Professor at the Department of Chemistry, University of Massachusetts Lowell. His research interests lie in the areas of design and synthesis of ultrafast broadband photoresponsive linear and nonlinear multiphoton energy absorptive fullereryl nanostructures and polycationic, nano-PDT drugs in combination of photoenergy, in one-photon absorptive 1PA-PDT and NIR two-photon absorptive 2PA-PDT, to kill multiantibiotic-resistant bacteria and cancer/tumor cells. He has published 269 peer-reviewed articles, book chapters, review articles, and awarded 39 patents. He was a chairman of several MRS symposia and a member of international advisory committee of ICSM. He was a member of editorial board and regional editor of two journals and is for one journal.



**Michael R. Hamblin, Ph.D.** is a Principal Investigator at the Wellman Center for Photomedicine at Massachusetts General Hospital, an Associate Professor of Dermatology at Harvard Medical School and is a member of the affiliated faculty of the Harvard-MIT Division of Health Science and Technology. His research interests lie in the areas of photodynamic therapy (PDT) for infections and cancer, and in low-level light therapy (LLLT) for wound healing, arthritis, traumatic brain injury and hair regrowth. He has published 250 peer-reviewed articles, over 150 conference proceedings, book chapters, has edited 3 major textbooks, and holds 8 patents. He is Associate Editor for 7 journals and serves on NIH Study Sections. In 2011 Dr Hamblin was honored by election as a Fellow of SPIE.

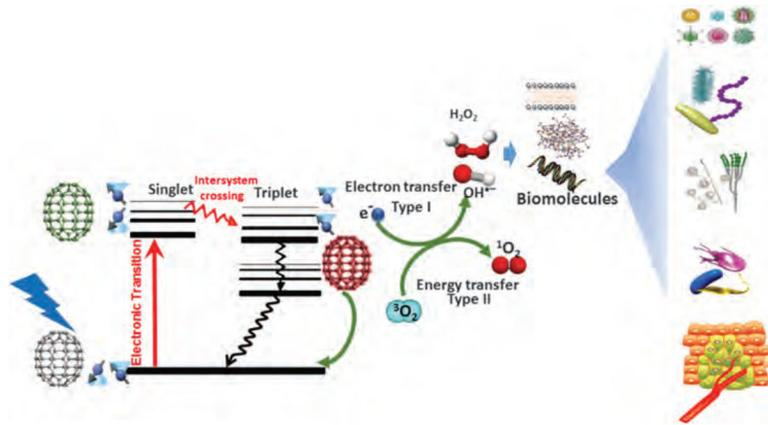


**Figure 1.**  
Schematic of PDT mediated by fullerenes.

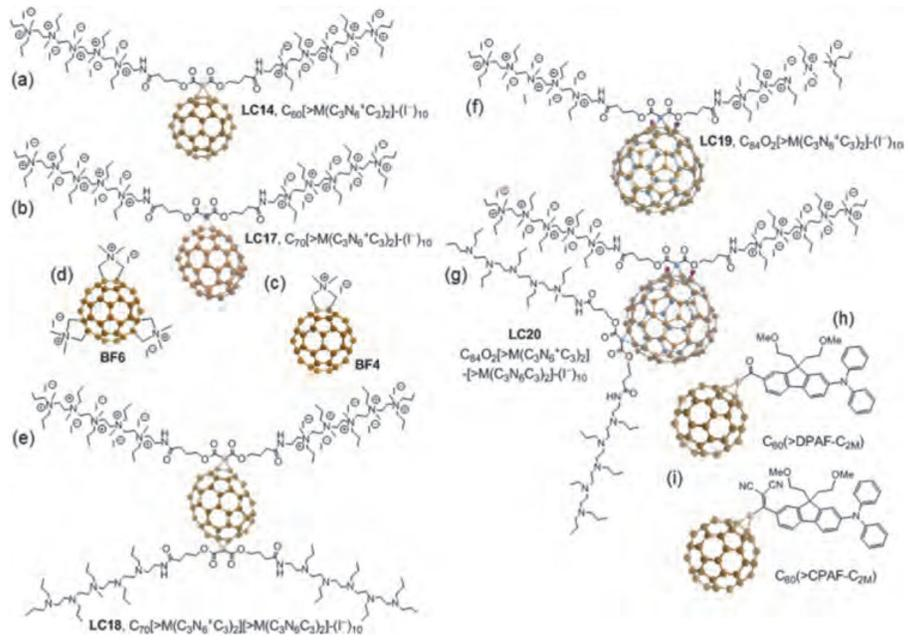


**Figure 2.**  
The chemical structure of fullerene derivatives applied in PDT studies.



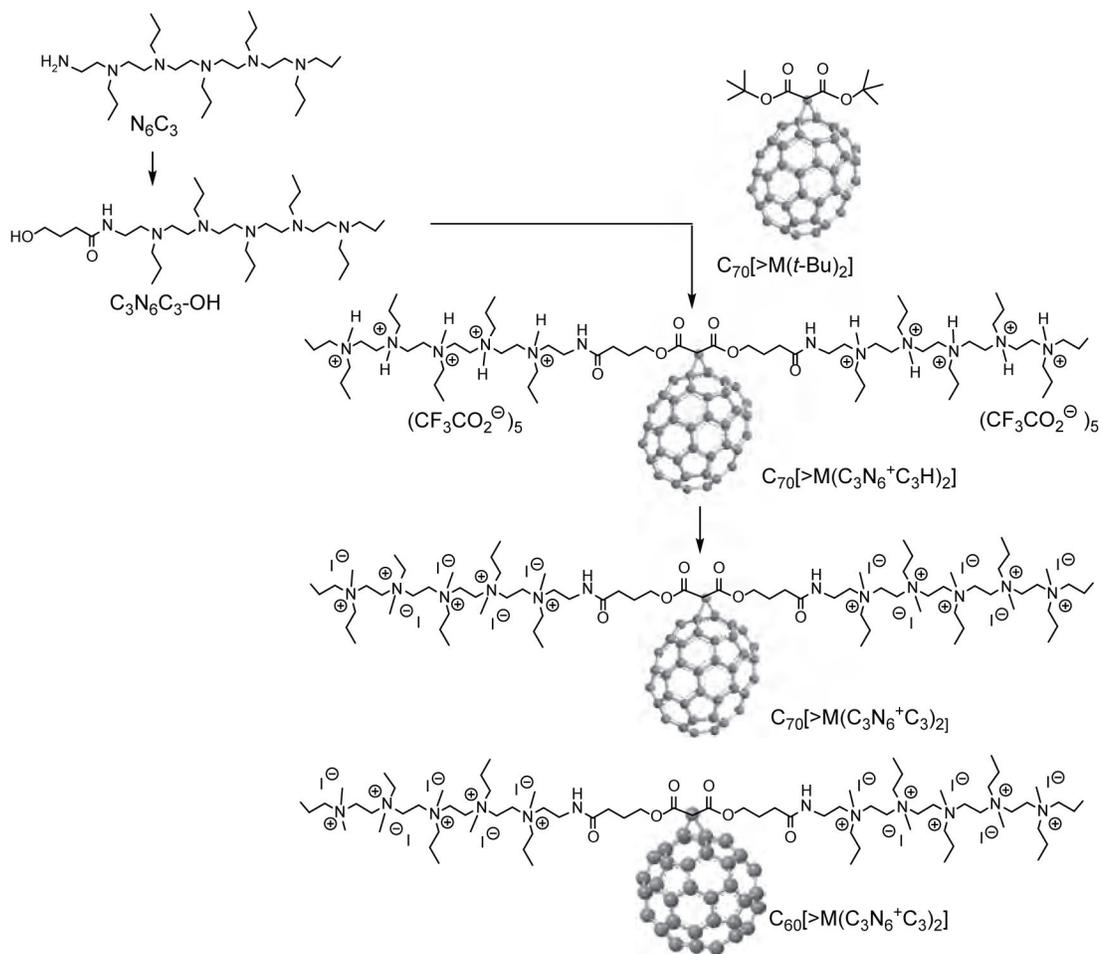


**Figure 4.**

Synthetic scheme for the preparation of C<sub>60</sub>[>M(C<sub>3</sub>N<sub>6</sub><sup>+</sup>C<sub>3</sub>)<sub>2</sub>] and C<sub>70</sub>[>M(C<sub>3</sub>N<sub>6</sub><sup>+</sup>C<sub>3</sub>)<sub>2</sub>].

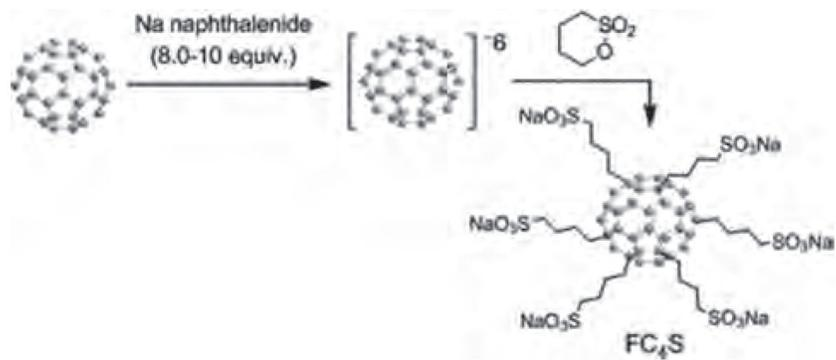


**Figure 5.**  
Synthesis of hexaanionic hexa(sulfo-*n*-butyl)-C<sub>60</sub> (FC<sub>4</sub>S).

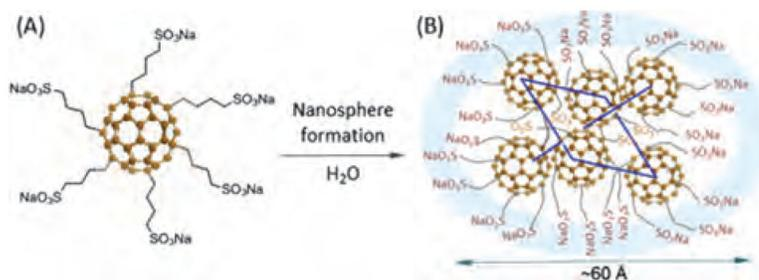


**Figure 6.** (A) Structure of hexa(sulfo-*n*-butyl) [60]fullerene (FC<sub>4</sub>S) and (B) a characterized FC<sub>4</sub>S-derived nanosphere formed in H<sub>2</sub>O discussed by Yu.<sup>85</sup>

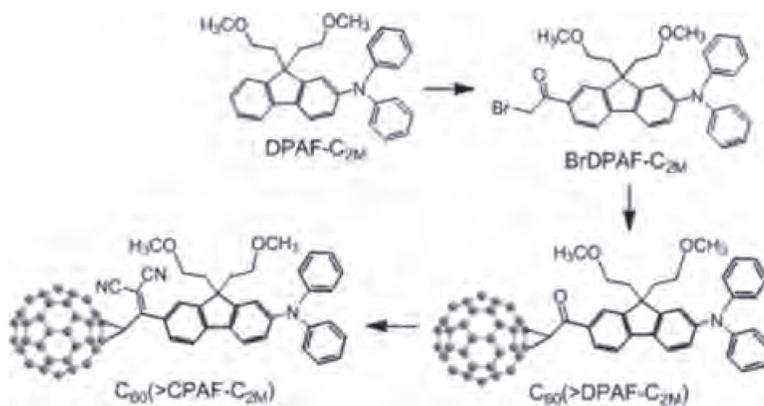


**Figure 7.** Synthetic method of C<sub>60</sub>(>CPAF-C<sub>2M</sub>) discussed by Chiang.<sup>73</sup>

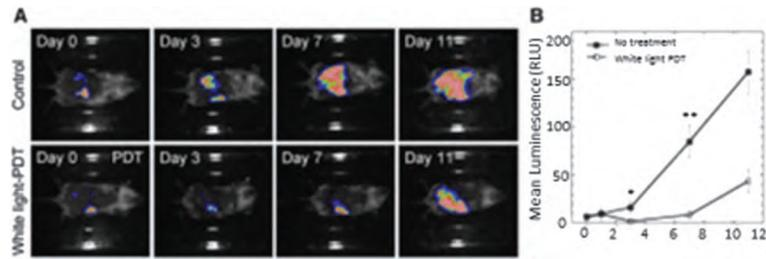


**Figure 8.**

(A) Bioluminescence imaging of CT26-Luc tumors growing in a representative control mouse (upper panel) and a representative IPPDT treated mouse (lower panel). (B) Quantitative analysis of bioluminescence dynamics in control and white light treated mice ( $n = 10$  per group). Reprinted with permission from [102], P. Mroz, et al., Intraperitoneal photodynamic therapy mediated by a fullerene in a mouse model of abdominal dissemination of colon adenocarcinoma. *Nanomedicine* 7, 965 (2011). © 2011, Future Science.

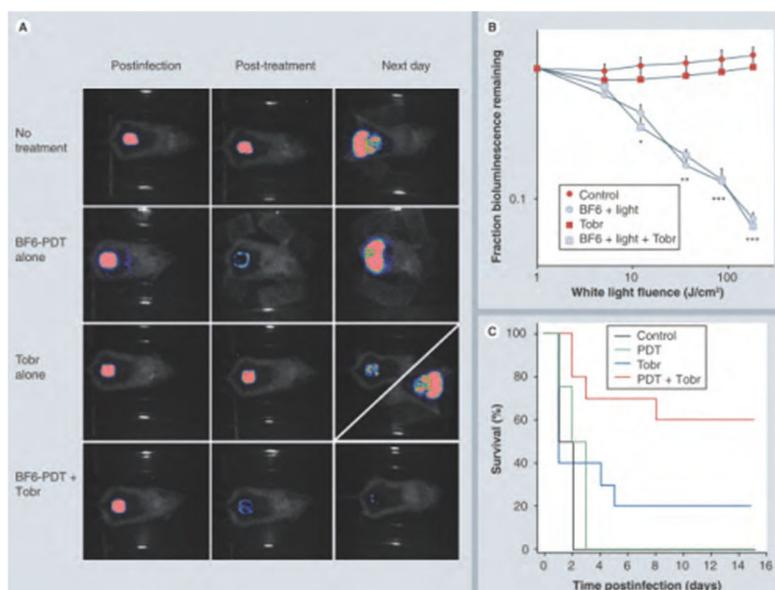


**Figure 9.** BF6-PDT and tobramycin treatment of *Pseudomonas aeruginosa* wound-infected mice. (A) Representative bioluminescence images of *P. aeruginosa*-infected mice (captured immediately postinfection, immediately post-treatment and 24 h post-treatment), receiving: no treatment (top row); treated with BF6-PDT alone ( $180 \text{ J/cm}^2$ ; second row); treated with Tobr alone ( $6 \text{ mg/kg}$  for 1 day; third row, diagonal panel 24 h post-treatment shows two possible outcomes); and treated with a combination of BF6-PDT and 1 day Tobr (bottom row). (B) Quantification of luminescence values from bioluminescence images (not shown) obtained during the PDT process, or at equivalent times for non-PDT mice. \*  $p < 0.05$ ; \*\*  $p < 0.01$ ; \*\*\*  $p < 0.001$ ; BF6 plus light (with and without Tobr) versus BF6 in dark and versus Tobr alone. (C) Kaplan–Meier survival curves for the groups of mice in Figure 4(A); no treatment control ( $n = 10$ ); PDT alone ( $n = 12$ ); Tobr alone ( $n = 2$ ); PDT plus Tobr ( $n = 10$ ). PDT: Photodynamic therapy; Tobr: Tobramycin. Reprinted with permission from [81], Z. Lu, et al., Photodynamic therapy with a cationic functionalized fullerene rescues mice from fatal wound infections. *Nanomedicine (Lond.)*, 5, 1525 (2010). © 2010, Future Science.

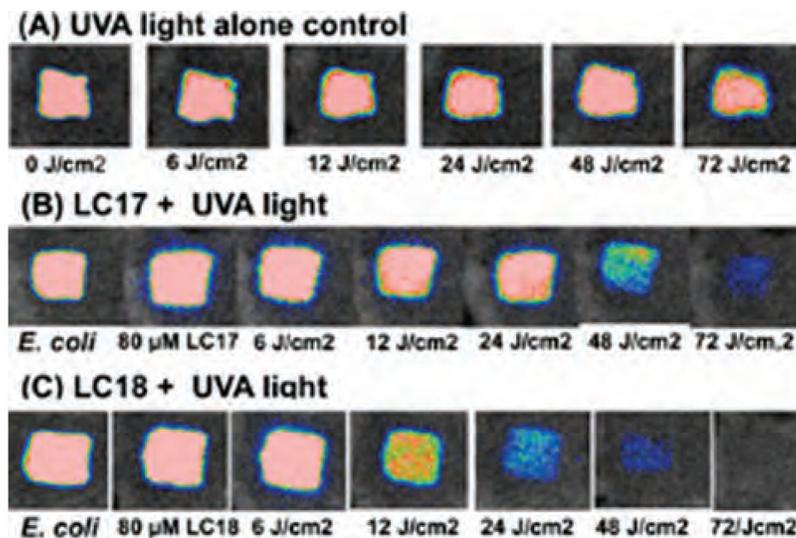


**Figure 10.**

Representative bioluminescence images from mice with *Escherichia coli* burn infections (day 0) and treated with successive fluences of photodynamic therapy or UVA light alone. (A) UVA control; (B) LC17 + UVA light; and (C) LC18+UVA light. There was no significant reduction in bioluminescence after application of either LC17 or LC18 without light exposure as a dark control. Reprinted with permission from [119], L. Huang, et al., Antimicrobial photodynamic therapy with decacationic monoadducts and bisadducts of [70]fullerene: *In vitro* and *in vivo* studies. *Nanomedicine (Lond.)* (2013).

© 2013, Future Science.

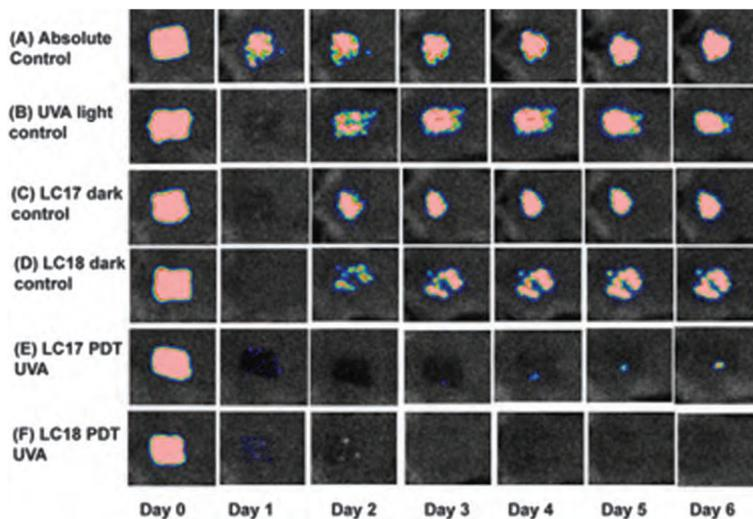


**Figure 11.**

Representative bioluminescence images from mice with *Acinetobacter baumannii* burn infections and treated with photodynamic therapy, UVA light alone or absolute control, captured day 0 (before photodynamic therapy) and then daily for 6 days. (A) Absolute control; (B) UVA control+15% DMA; (C) LC17+15% DMA; (D) LC18+15% DMA; (E) LC17+15% DMA+UVA light; and (F) LC18+15% DMA+UVA light. Reprinted with permission from [119], L. Huang, et al., Antimicrobial photodynamic therapy with decacationic monoadducts and bisadducts of [70]fullerene: *In vitro* and *in vivo* studies. *Nanomedicine (Lond.)* (2013).

© 2013, Future Science.